Economic Geology, v. 94, pp. 455-473

Economic Geology

BULLETIN OF THE SOCIETY OF ECONOMIC GEOLOGISTS

VOL. 94 June–July 1999 NO. 4

Quantitative Relationships among Giant Deposits of Metals

PETER LAZNICKA[†,*]

Department of Geological Sciences, University of Manitoba, Winnipeg, Manitoba, Canada R3T 2N2

Abstract

Metallogenic studies that try to identify the geochemical fluxes of metals in the lithosphere leading to ore formation have a higher sensitivity when the traditional mining data, based on grades and tonnages, are normalized to crustal element abundances, and derivative units such as clarke of concentration and tonnage accumulation index are used. This technique has been applied to the world-class deposits of all industrial metals, i.e., to 34 metals plus the rare earth elements and platinoid groups. The lower magnitude limits for inclusion in the giant and supergiant categories (ore metal content in a deposit/metal clarke > 1×10^{11} metric tons (t) and 10^{12} t of average crustal material, respectively) have been established for each metal. There are, presently, 486 giant and 61 supergiant metal accumulations of the various metals in 446 deposits and districts. A single deposit and/or district, such as the Olympic Dam Cu-U-Au-REE-Fe deposit, could be the site of a giant accumulation of more than one metal. Cu with 103 giant accumulations followed by Au (99), Pb (55), Mo (41), Sb (24), and Sn (22) are the most superaccumulated metals, whereas 11 metals entirely lack giant deposits. Although this is partly influenced by economic factors, such as low demand and price, the main cause is the geochemical behavior of metals, especially the trace metals compatibilities at the various stages of crustal evolution.

Porphyry Cu-Mo deposits have the greatest number of giant accumulations among the popular ore deposit types (90), followed by sedimentary exhalative Zn-Pb-Ag (23), volcanogenic massive sulfides (22), stockwork Mo (17), epithermal Au-Ag veins (13), and Broken Hill-type Pb-Zn-Ag (12). In terms of origin, the greatest number of giant deposits is among the mesothermal Cu deposits (67), which reflect the porphyry Cu-Mo preeminence, followed by mesothermal Au (61), mesothermal Mo (39), mesothermal Sb (22), mesothermal Pb (19), and sediment-hosted Cu deposits at redox interfaces (19). As a class, the mesothermal epigenetic deposits account for 271 giant metal accumulations, which represents 52 percent of the entire database. Hydrothermal deposits including exhalative and epithermal deposits possess 333 giant representatives, or 63.5 percent. Other genetic families of ore deposits, including precipitates from less than 150°C hot hydrous fluids (59 giant deposits), orthomagmatic deposits (40), sedimentary deposits (39), and weathering-generated deposits (14), are less significant. An astonishing 446 giant metal accumulations (92.5%) thus relied on water as the principal agent of formation.

Of the giant deposits genetically associated with magmatism, the metaluminous granodiorite-quartz monzonite suite at subductive margins is related to most giant deposits (98, or 19%). Second in importance is the high potassium granite suite (23 giant deposits). Carbonatites, with only about 350 occurrences known worldwide, are the most striking rare magmatic hosts to giant deposits. Five carbonatites host giant or supergiant deposits and an additional 11 carbonatites host large deposits (i.e., tonnage accumulation index > 1×10^{10} t), so there is a 4.5 percent chance that any newly discovered carbonatite will host a large or giant deposit. The major period of preserved giant deposit accumulation occurred during lower-middle Tertiary (103 giant deposits or 20% of the total), followed by middle-upper Tertiary (59 giant deposits), Jurassic (39 giant deposits), Carboniferous (37 giant deposits), and Paleoproterozoic (33 giant deposits). The predominantly young age of mineralization indicates that shallow crustal depths or subsiding subaqueous and subaerial depositories provide the most favorable milieu for superaccumulation of many metals but, on the other hand, are vulnerable to removal by erosion.

Introduction

THE INFORMAL term "world-class mineral deposit," applied to ore deposits with an exceptionally large tonnage of economically recoverable metals, is widespread in the present literature on economic and resource geology (Cox and Singer, 1986; Whiting et al., 1993; Clark, 1995; Keith and Swan, 1996). When quantitatively defined, the world-class designation applies to the upper 10 percent deposits in terms of contained metal (Singer, 1995). The term attests to an exceptional economic benefit these deposits provide, or potentially provide, and consequently this class of deposits is eagerly sought by the industry. This, in turn, drives research into the geologic nature of the world-class deposits.

[†] Email: Plaznicka@amf.com.au

*Present address: Australian Mineral Foundation, Glenside, South Australia 5065, Australia.

Vol. 94, 1999, pp. 455–474
0361-0128/99/2065/455-20 $6.00

World-class deposits are heterogeneous in nature. A typical recent example is the Olympic Dam Cu-U-Au deposit, South Australia (Oreskes and Einaudi, 1990; Reeve et al., 1990) that has a published reserve of about 2 bt of ore with the contained Cu, U, Au, and REE worth about $162 billion at the present prices. Olympic Dam is a member of the world-class league with respect to three metals. It is the fifth largest copper accumulation in the world (32 Mt Cu) whose grade of 1.6 percent Cu is intermediate between the porphyry coppers and the rich strata-bound deposits of the African Copperbelt. It is the world's single largest uranium accumulation (1.088 Mt U) that contains about 2.2 times more uranium than the rest of the Australian deposits taken together, or about 120 percent of the past production and remaining reserves of all uranium deposits in Canada and about 16 percent of the world's U reserves.

There are several hundred metallic deposits (i.e., those with highly concentrated ore metals) recorded worldwide that are comparable with Olympic Dam in being single, relatively homogeneous, continuous, and clearly outlined exceptional accumulations of metals in concentrations that are close to, or exceed, the world's average ore grade calculated for each metal. Their value of metals in ground exceeds $1 billion for each deposit. In some cases this is augmented by several nonmetallics such as phosphates and vermiculite (Palabora), barite (Red Dog), sulfur, and others. The world-class status at a locality has been achieved by a single metal (e.g., Kalgoorlie: Au, Almaden: Hg, Climax: Mo), two metals (e.g., Chuquicamata: Cu and Mo, Grasberg: Cu and Au), three metals (e.g., Broken Hill, New South Wales: Pb, Zn, and Ag), or even four or more metals (e.g., Mount Isa: Pb, Zn, Ag, and Cu). The exceptionally large metals repositories are rare; there are less than 500 entries worldwide based on the definition outlined below, and they are not only economically exciting but also scientifically interesting. What is needed is a way to mutually compare, contrast, and rank the exceptionally large accumulations of the various metals that reside in deposits of many types and ages in order to find out what causes them to form as a class, if anything; what geotectonic setting they favor, if any; what can they tell us about the efficiency of geologic processes, geochemical sinks and barriers, time constraints; where might be the giant deposits of the future. This paper attempts to provide answers to some of these questions.

The Database

Quantitative conclusions reached in this paper are based on GIANTDEP, an unpublished database that stores data on the world's largest geologic accumulations of industrial metals (Laznicka, 1998). In this database each entry represents an exceptional accumulation of one ore metal only in an orebody, ore deposit, ore field, district, or basin, identified as a locality. In most cases there is one entry per locality but if one locality stores exceptional tonnages of more than one metal, it is entered two or more times (Table 1). The number of entries in GIANTDEP is thus greater than the number of localities.

The data come from multilingual literature supplemented by oral communications, some unpublished reports, and by site visits at about 70 percent of the deposits considered herein. The metal content tonnages represented here are close to the geologic reserves, defined here as the total content of industrial metals in a deposit before mining above a certain cut-off grade determined by economic conditions.

TABLE 1. Deposits and Districts that Contain Exceptionally Large Accumulations of Two or More Metals

Metals	Number of localities	Example locality	Metals	Number of localities	Example locality
Two metals			Three metals		
Au, Ag	1	Pachuca, Mexico	Ag, Pb, Zn	6	Sullivan, Canada
Ag, Cu	2	Lubin (Kupferschiefer), Poland	Ag, Pb, Au	1	Beregovo, Ukraine
Ag, Pb	6	Santa Eulalia, Mexico	Ag, Cu, Mo	1	Butte, Montana, U.S.A.
Ag, Sn	3	Potosi, Bolivia	Ag, Cu, Zn	1	Kidd Creek, Canada
Ag, Zn	1	Rajpura-Dariba, India	Au, Cu, Mo	2	Petaquilla, Panama
As, V	1	Kerch Fe basin, Ukraine	Bi, Sn, W	1	Shizhouyuan, China
Au, As	2	Vasil'kovskoye, Kazakhstan	Cu, As, Se	1	Rio Tinto ore field, Spain
Au, Cu	13	Grasberg, Indonesia	Cu, Ni, PGE	2	Sudbury Complex, Ontario[1]
Au, Te	2	Cripple Creek, Colorado, U.S.A.	Cu, U, Au	1	Olympic Dam, South Australia
Au, U	1	Witwatersrand basin, South Africa[1]	Pb, Cd, As	1	Tsumeb, Namibia
Bi, Sn	1	Gejiu, China	PGE, Ni, Au	2	Merensky Reef, South Africa
Cr, PGE	2	Great Dyke, Zimbabwe[1]	Ti, Fe, V	1	Bushveld magnetitites, South Africa
Cu, Mo	10	Chuquicamata, Chile	W, Bi, Te	1	Verkhnye Qairakty, Kazakhstan
Cu, Co	1	Katanga (Shaba) copper belt, Congo	Zr, Nb, REE	1	Ilimaussaq Complex, Greenland[1]
Cu, Ni	2	Jinchuan, China			
Fe, Mn	1	Urucum (Corumba), Brazil	Four metals		
Fe, V	1	Bakchar ore field, Russia			
Mo, U	1	Billingen (alum shale), Sweden	Ag, Mo, Cu, Au	1	Bingham Canyon porphyry, U.S.A.
Nb, REE	1	Bayan Obo, China	Pb, Zn, Ag, Cu	1	Mount Isa, Australia
Nb, Th	1	Araxa, Brazil	Zn, Pb, Ag, Bi	1	Brunswick 6, 12, Canada
Nb, Zr	1	Lovozero Complex, Russia[1)]	REE, Y, Nb, Sc	1	Tomtor, Anabar massif, Russia
Ni, Co	1	New Caledonia laterites			
Pb, Sb	1	Bawdwin, Myanmar (Burma)	Five metals		
Pb, Zn	8	Century, Australia	Zn, Pb, Ag, As, Sb	1	Cerro de Pasco, Peru

[1] Cumulative tonnage of several deposits in a mineralized complex

Many tonnage figures here are direct quotations from the literature. Other figures have been calculated by adding the metal tonnages in past production, metals present in remaining reserves, and metals lost during production or left in ground. In the remainder of entries metal tonnages have been reconstructed by extrapolation from incomplete data and in a few cases estimates were made based on comparison with better-documented deposits. The problems of data capture from the literature are discussed in Laznicka (1985) and most of the difficult cases come from countries such as China and the former U.S.S.R. where, at least until recently, the production and reserve figures were confidential for most mineral commodities.

The selection of entries for the present study is influenced by three additional considerations: (1) resources, (2) nonconventional ores, and (3) definition of locality.

1. Metal resources are not included in GIANTDEP, with the exception of calculated ore metal contents in the Bushveld magmatic stratiform ore horizons. This contrasts with Singer (1995) who does include resources, hence Singer's ore and metal tonnages are higher.

2. Classical metal ores are natural materials that have high to extremely high concentration factors of metals in respect to the clarke values. The classical ore deposits are delineated and their limits are based either on a sharp-grade decrease or on an assay boundary. Since approximately World War II, new, nontraditional metal sources (Barton, 1983) have entered production or a technology has become available for nonconventional metal recovery from such materials (Table 2). Metal concentration factors of the nonconventional raw materials range from several tens (e.g., Li dissolved in the Salar de Atacama brine; Ferrell, 1985) through one (e.g., Ti in the Stradbrooke Island, Queensland, heavy mineral sands; Wallis and Oakes, 1990) to negative (e.g., Mg recovered from seawater; Kramer, 1985) and many of the material bodies are open ended or their limits based on political or property boundaries. The nontraditional ores render obsolete many classical concepts of metallogeny and they require special treatment. Because the present study emphasizes geochemical concentration peaks, it is limited to the classical ores and the very low grade materials listed in Table 2 are not considered. The study does, however, include several geologic bodies such as the Bushveld titanomagnetite layer which, although not presently economic as a whole, constitutes a striking metallogenic anomaly.

3. Most localities included here are well-delineated single deposits (e.g., Olympic Dam, Climax, El Teniente). Others are zones of coalescing orebodies of the same type (Broken Hill Pb-Zn-Ag, N.S.W.), complexes in which originally continuous ore layers are now separated by younger intrusions or by erosion (Merensky Reef in the Bushveld Complex, ironstone seams in the West Siberian basin), or districts and basins in which numerous deposits of the same type, age, and probably derivation are physically separated by barren gaps (the Witwatersrand basin Au-U, the Boke-Gaoual lateritic bauxite terrane in Guinea). Because of the global nature of this study, single deposits are sometimes treated jointly with mineralized objects in which the ore metals reside in a number of orebodies, some of which (or none of which) are of the giant magnitude but which together constitute a giant interrelated genetic system. This is a prevalent practice in global metallogenic studies (Routhier, 1980; Meyer, 1981; Cox and Singer, 1986; Singer, 1995).

Ore Deposit Data in Geochemical Context

Although the metal tonnage and grade data for metallic deposits published by industry and governments can be applied directly to quantitatively support numerous research conclusions in metallogeny, it is often advantageous to use derivative units normalized to the clarke values, a philosophy suggested for the first time in the 1960s (McKelvey, 1960; Erickson, 1973). Derivative units are relatively free of economic bias, but they depend on the clarke values that vary with different authorities. Clarke values for continental crust estimated by Wedepohl (1995), illustrated here by several trace metals, are 56 ppm Ni, 25 ppm Cu, 14.8 ppm Pb, 1.7 ppm U, and 2.5 ppb Au. Corresponding values calculated by Rudnick and Fountain (1995) are 51 ppm Ni, 24 ppm Cu, 12.6 ppm Pb, and 1.42 ppm U (no gold). Alternatively, Taylor and McLennan (1995) credit their "bulk continental crust" with 105 ppm Ni, 75 ppm Cu, 8.0 ppm Pb, 0.91 ppm U, and 3.0 ppb Au. The discrepancy in the crucial metallogenic elements such as Ni is about 200 percent, Cu 300 percent, Pb under 200 percent, and U under 200 percent. Relative to other studies, Taylor and McLennan (1995) gave more weight to the mafic component in the lower crust. In this study the clarke values of Wedepohl (1995) are used.

The principal measure of the relative element concentration is concentration factor (or clarke of concentration; Fersman, 1933), defined as the average ore grade/clarke of the ore metal. A measure of the relative magnitude of ore metal accumulation is the tonnage accumulation index (Laznicka, 1983), defined as the quantity of a metal in the mineralized object/clarke of that metal. Tonnage accumulation index corresponds to the tonnage of average crust that would contain the equivalent tonnage of the metal in the geologic reserve of a given ore deposit. Tonnage accumulation index is an indicator of the magnitude of geochemical efficacy of an ore generation process or setting and also of metallogenic uniqueness. It provides a common denominator for comparison and ranking of magnitudes of accumulation of metals with highly contrasting clarke values, such as gold, copper, or iron. Tonnage accumulation index can thus determine quantitatively which of two (or more) deposits, one of gold and the other of copper, is more geochemically exceptional in terms of efficiency of the ore-forming process and/or setting.

Laznicka (1983) set the lower limit of giant metal accumulations at tonnage accumulation index = 1×10^{11} t of the average crust equivalent. Supergiant accumulations start at tonnage accumulation index = 1×10^{12} t and large accumulations at 1×10^{10} t. Table 3 lists the minimum tonnages of metals in ore deposits necessary to be included in the giant and supergiant classes. These metal tonnages are different for each metal because the clarke value is different for each metal; for example, a giant manganese deposit has the lower limit of 7.2×10^{7} t Mn in ore, a giant copper deposit starts at 2.5×10^{6} t Cu in ore, and a giant gold accumulation has to contain in excess of 250 t Au in ore. The problem of the enormous range of tonnage magnitudes within one division of a log scale (e.g., the 1983 vintage giant copper deposit, defined

TABLE 2. Selected Non-Traditional Producers, Past Producers, and Investigated Sources of Industrial Metals

Metal source	Area, locality	Distribution of metal substance	Grade	Clarke of concentration	Reserve resource	Tonnage accumulation index	Industrial utilization	Reference
Mg recovered from seawater	World ocean	Mg in $MgCl_2$ dissolved in sea water	0.13% Mg	6.6×10^{-1}	$N \times 10^{13}$	$N \times 10^{14}$	Active production, six operations in U.S.A. alone in 1980s	Kramer (1985)
Li recovered from playa brine	Salar de Atacama, Chile	Li dissolved in brine interstitial to salt	0.14% Li	7.8×10^{1}	1.35×10^{6}	7.5×10^{10}	Active production, world's largest supplier of Li, $LiCl_2$	Ferrell (1985)
W, As recoverable from playa brine	Searles Lake, California, U.S.A.	W dissolved in brine interstitial to salt (with As)	32 ppm W; 100 ppm As	W, As 3.2×10^{1} 5.9×10^{1}	W, As 6.8×10^{4} 2.1×10^{5}	W, As 6.8×10^{10} 3.5×10^{11}	Possible by-product of Na_2CO_3, B, Li production	Smith (1979)
V recovered from petroleum	Venezuela and other countries	V resides in hydrocarbons, concentrates in ashes	100–464 ppm V	1–4.64	9.0×10^{3}	9×10^{7}	Recovered in several local and overseas refineries	Kuck (1985)
Hg recovered from natural gas	Groningen gas field, Netherlands; former E. Germany	Hg vapors in gas from reservoirs in Zechstein	2 mg Hg/m^3	2×10^{-2}	3.0×10^{3}	7.5×10^{10}	Recovered in some gas scrubbing plants	Ozerova (1981)
V recovered from tar sands	Athabasca oil sands area, Alberta	Dispersed V > Ni in bitumen matrix to Cretaceous sand	240 ppm V	2.4	3.0×10^{6}	3.0×10^{10}	Partial V recovery as by-product of bitumen processing	Scott et al. (1954)
Al by-product of oil shale processing	Piceance basin, Colorado	Al in authigenic dawsonite and nordstrandite in shale	2.15% Al	3.7×10^{0}	3.1×10^{9}	3.9×10^{10}	Investigated as potential oil by-product	Smith and Milton (1966)
Ge recovered from residua after coal burning	British Carboniferous coals and elsewhere	Trace Ge partitions into ash and flue dust up to a maximum of 2% Ge	7 ppm Ge mean	5.0	2.0×10^{5}	1.4×10^{11}	Industrial recovery in one plant in UK, 1950–1970	Paone (1970)
U as by-product of phosphorite processing	Florida Phosphate province, Miocene-Pliocene	Trace U in fluorapatite and enriched in Al phosphates	85 ppm U mean	5.7×10^{1}	1.5×10^{6}	9×10^{11}	By-product of H_3PO_3 production, capacity 1,070 t U/yr in 1980s	Fountain and Hayes (1979)
Ga recovered from bauxite residua	Jamaica bauxite province; elsewhere	Ga accumulates in red mud processing residuum	50 ppm Ga mean	3.33	1.0×10^{4}	6.8×10^{8}	Investigated as by-product of red mud waste reclamation	Petkof (1985)
Ti, Zr in low-grade dune sands	North Stradbrooke Island dunes, Queensland	Ilmenite > rutile, zircon in heavy mineral fraction; 1.5–2% heavies, cutoff 0.75%	0.5% Ti 0.18% Zr	1.25 Ti 9.00 Zr	4.8×10^{6} 4.6×10^{5}	1.2×10^{9} 2.3×10^{9}	Profitably mined and processed; low-cost, environmentally friendly	Wallis and Oakes (1990)
Mn in nodules from Cretaceous shale	Chamberlain, South Dakota; area 240 km × 180 m	Diagenetic nodules with 15.5% Mn make up 5.5% of 13 m shale interval	0.85% Mn	1.2×10^{1}	1.1×10^{7}	1.5×10^{10}	Investigated as wartime emergency strategic resource	Pesonen et al. (1949)

TABLE 3. Crustal Metal Abundances (Clarkes), and Limits and Ranges of Magnitude Classes (Expressed in Exceptional Metal Accumulations)

Metal	Clarke (ppm)	Large deposits (t) Low	Large deposits (t) Mid	Large deposits (t) High	Giant deposits (t) Low	Giant deposits (t) Mid	Giant deposits (t) High	Supergiant deposits (t) Low	Supergiant deposits (t) Mid	Supergiant deposits (t) High
Al	8.0×10^4	8.0×10^8	3.2×10^9	5.6×10^9	8.0×10^9	3.2×10^{10}	5.6×10^{10}	8.0×10^{10}	3.2×10^{11}	5.6×10^{11}
Fe	4.3×10^4	4.3×10^8	1.7×10^9	3.0×10^9	4.3×10^9	1.7×10^{10}	3.0×10^{10}	4.3×10^{10}	1.7×10^{11}	3.0×10^{11}
Ti	4.0×10^3	4.0×10^7	1.6×10^8	2.8×10^8	4.0×10^8	1.6×10^9	2.8×10^9	4.0×10^9	1.6×10^{10}	2.8×10^{10}
Mn	7.2×10^2	7.2×10^6	2.9×10^7	5.0×10^7	7.2×10^7	2.9×10^8	5.0×10^8	7.2×10^8	2.9×10^9	5.0×10^9
Zr	2.0×10^2	2.0×10^6	8.0×10^6	1.4×10^7	2.0×10^7	8.0×10^7	1.4×10^8	2.0×10^8	8.0×10^8	1.4×10^9
REE	1.5×10^2	1.5×10^6	6.0×10^6	1.1×10^7	1.5×10^7	6.0×10^7	1.1×10^8	1.5×10^8	6.0×10^8	1.1×10^9
Cr	1.3×10^2	1.3×10^6	5.2×10^6	9.1×10^6	1.3×10^7	5.2×10^7	9.1×10^7	1.3×10^8	5.2×10^8	9.1×10^8
V	1.0×10^2	1.0×10^6	4.0×10^6	7.0×10^6	1.0×10^7	4.0×10^7	7.0×10^7	1.0×10^8	4.0×10^8	7.0×10^8
Zn	6.5×10^1	6.5×10^5	2.6×10^6	4.6×10^6	6.5×10^6	2.6×10^7	4.6×10^7	6.5×10^7	2.6×10^8	4.6×10^8
Ni	5.5×10^1	5.5×10^5	2.2×10^6	3.9×10^6	5.5×10^6	2.2×10^7	3.9×10^7	5.5×10^7	2.2×10^8	3.9×10^8
Cu	2.5×10^1	2.5×10^5	1.0×10^6	1.8×10^6	2.5×10^6	1.0×10^7	1.8×10^7	2.5×10^7	1.0×10^8	1.8×10^8
Co	2.4×10^1	2.4×10^5	9.6×10^5	1.7×10^6	2.4×10^6	9.6×10^6	1.7×10^7	2.4×10^7	9.6×10^7	1.7×10^8
Y	2.4×10^1	2.4×10^5	9.6×10^5	1.7×10^6	2.4×10^6	9.6×10^6	1.7×10^7	2.4×10^7	9.6×10^7	1.7×10^8
Nb	1.9×10^1	1.9×10^5	7.6×10^5	1.3×10^6	1.9×10^6	7.6×10^6	1.3×10^7	1.9×10^7	7.6×10^7	1.3×10^8
Li	1.8×10^1	1.8×10^5	7.2×10^5	1.3×10^6	1.8×10^6	7.2×10^6	1.3×10^7	1.8×10^7	7.2×10^7	1.3×10^8
Sc	1.6×10^1	1.6×10^5	6.4×10^5	1.1×10^6	1.6×10^6	6.4×10^6	1.1×10^7	1.6×10^7	6.4×10^7	1.1×10^8
Ga	1.5×10^1	1.5×10^5	6.0×10^5	1.1×10^6	1.5×10^6	6.0×10^6	1.1×10^7	1.5×10^7	6.0×10^7	1.1×10^8
Pb	1.5×10^1	1.5×10^5	6.0×10^5	1.1×10^6	1.5×10^6	6.0×10^6	1.1×10^7	1.5×10^7	6.0×10^7	1.1×10^8
Th	8.5	8.5×10^4	3.4×10^5	6.0×10^5	8.5×10^5	3.4×10^6	6.0×10^6	8.5×10^6	3.4×10^7	6.0×10^7
Cs	3.4	3.4×10^4	1.4×10^5	2.4×10^5	3.4×10^5	1.4×10^6	2.4×10^6	3.4×10^6	1.4×10^7	2.4×10^7
Be	2.4	2.4×10^4	9.6×10^4	1.7×10^5	2.4×10^5	9.6×10^5	1.7×10^6	2.4×10^6	9.6×10^6	1.7×10^7
Sn	2.3	2.3×10^4	9.2×10^4	1.6×10^5	2.3×10^5	9.2×10^5	1.6×10^6	2.3×10^6	9.2×10^6	1.6×10^7
As	1.7	1.7×10^4	6.8×10^4	1.2×10^5	1.7×10^5	6.8×10^5	1.2×10^6	1.7×10^6	6.8×10^6	1.2×10^7
U	1.7	1.7×10^4	6.8×10^4	1.2×10^5	1.7×10^5	6.8×10^5	1.2×10^6	1.7×10^6	6.8×10^6	1.2×10^7
Ge	1.4	1.4×10^4	5.6×10^4	9.8×10^4	1.4×10^5	5.6×10^5	9.8×10^5	1.4×10^6	5.6×10^6	9.8×10^6
Ta	1.1	1.1×10^4	4.4×10^4	7.7×10^4	1.1×10^5	4.4×10^5	7.7×10^5	1.1×10^6	4.4×10^6	7.7×10^6
Mo	1.1	1.1×10^4	4.4×10^4	7.7×10^4	1.1×10^5	4.4×10^5	7.7×10^5	1.1×10^6	4.4×10^6	7.7×10^6
W	1.0	1.0×10^4	4.0×10^4	7.0×10^4	1.0×10^5	4.0×10^5	7.0×10^5	1.0×10^6	4.0×10^6	7.0×10^6
Tl	5.0×10^{-1}	5.0×10^3	2.0×10^4	3.5×10^4	5.0×10^4	2.0×10^5	3.5×10^5	5.0×10^5	2.0×10^6	3.5×10^6
Sb	3.0×10^{-1}	3.0×10^3	1.2×10^4	2.1×10^4	3.0×10^4	1.2×10^5	2.1×10^5	3.0×10^5	1.2×10^6	2.1×10^6
Se	1.2×10^{-1}	1.2×10^3	4.8×10^3	8.4×10^3	1.2×10^4	4.8×10^4	8.4×10^4	1.2×10^5	4.8×10^5	8.4×10^5
Cd	1.0×10^{-1}	1.0×10^3	4.0×10^3	7.0×10^3	1.0×10^4	4.0×10^4	7.0×10^4	1.0×10^5	4.0×10^5	7.0×10^5
Bi	8.5×10^{-2}	8.5×10^2	3.4×10^3	6.0×10^3	8.5×10^3	3.4×10^4	6.0×10^4	8.5×10^4	3.4×10^5	6.0×10^5
Ag	7.0×10^{-2}	7.0×10^2	2.8×10^3	4.9×10^3	7.0×10^3	2.8×10^4	4.9×10^4	7.0×10^4	2.8×10^5	4.9×10^5
In	5.0×10^{-2}	5.0×10^2	2.0×10^3	3.5×10^3	5.0×10^3	2.0×10^4	3.5×10^4	5.0×10^4	2.0×10^5	3.5×10^5
Hg	4.0×10^{-2}	4.0×10^2	1.6×10^3	2.8×10^3	4.0×10^3	1.6×10^4	2.8×10^4	4.0×10^4	1.6×10^5	2.8×10^5
PGE	1.3×10^{-2}	1.3×10^2	5.2×10^2	9.1×10^2	1.3×10^3	5.2×10^3	9.1×10^3	1.3×10^4	5.2×10^4	9.1×10^4
Te	5.0×10^{-3}	5.0×10^1	2.0×10^2	3.5×10^2	5.0×10^2	2.0×10^3	3.5×10^3	5.0×10^3	2.0×10^4	3.5×10^4
Au	2.5×10^{-3}	2.5×10^1	1.0×10^2	1.8×10^2	2.5×10^2	1.0×10^3	1.8×10^3	2.5×10^3	1.0×10^4	1.8×10^4
Re	4.0×10^{-4}	4.0×10^0	1.6×10^1	2.8×10^1	4.0×10^1	1.6×10^2	2.8×10^2	4.0×10^2	1.6×10^3	2.8×10^3

Clarke values after Wedepohl (1995), metals arranged by decreasing clarkes

on the clarke values of Taylor, 1964, had a range from 5.5 to 55 Mt Cu) was criticized by Clark (1993) who offered an alternative terminology applicable, unfortunately, to copper deposits only. The problem has been rectified here by subdividing each log interval of values into three equal portions (thirds) that are referred to as "low," "mid," and "high." So a 733 t Au deposit such as Cripple Creek would be a low giant, a 1,600 t Au goldfield like Kalgoorlie would be a mid giant, and the 2,100 t Au Grasberg-Dalam complex would be a high giant. The 6,500 t Au Welkom Basal reef would be a supergiant.

The Giant Metal Accumulations

The industrial trend toward globalization and production of goods in a relatively small number of large, mass-producing facilities capable of supplying the rest of the world has made a significant impact on the resources industry. The bulk mineable deposits of exceptional size, even of lower than normal grade, increasingly affect the global metal supply, corporate profitability, prices, and international politics. Singer (1995) calculated that the world-class deposits store over 86 percent of the world's gold, 79 percent of silver, 84 percent of copper, 71 percent of zinc, and 73 percent of lead. The share of single deposits, districts, or complexes is even more striking. The Bushveld Complex contains about 48 percent of the world's chromite, 46 percent of platinum metals in the Merensky reef only, and 41 percent of vanadium in the Main magnetitite seam only. The Central Rand Group in the Witwatersrand basin accounts for about 63,000 t of the world's gold recorded in published past production and remaining reserves data and more if unpublished estimates are included. Tables 4 and 5 and Figure 1 provide a survey of the world's ore metals reserves and the share of the global metal supply held by the exceptionally well endowed localities. Figure 2 shows the approximate locations of the largest deposits or districts of each ore metal.

TABLE 4. Global Endowment of Ore Metals and Share of the Largest Deposits

Metal	Total production (t)[1]	Endowment minimum (t)[2]	Endowment maximum (t)[3]	Largest deposit/district	Object	Metal content (t)[4]	Percent of minimum endowment[5]	Percent of maximum endowment[6]
Al	5.05×10^8	1.10×10^{10}	1.20×10^{10}	Boke-Gaoual, Guinea	Area	3.88×10^9	35.27	32.33
Fe	3.40×10^{10}	1.50×10^{11}	1.00×10^{13}	Alegria, Brazil	Deposit	6.20×10^{10}	41.33	0.62
Ti	1.53×10^8	9.50×10^9	1.20×10^{10}	Bushveld main magnetite seam, South Africa	Unit	2.88×10^9	30.32	24.00
Mn	8.35×10^8	5.63×10^9	7.70×10^9	Kalahari-Mamatwan, South Africa	Deposit	4.19×10^9	74.42	48.16
Zr	1.86×10^7	4.45×10^8	4.70×10^8	Lovozero eudialyte lujavrite unit, Russia	Unit	2.10×10^8	47.19	44.68
REE	1.04×10^6	1.12×10^8	2.80×10^8	Tomtor, Anabar Shield, Russia	Deposit	4.00×10^7	35.71	14.29
Cr	4.30×10^8	7.23×10^9	9.20×10^9	Bushveld chromitite seams, South Africa	Unit	3.47×10^9	48.00	37.72
V	8.61×10^5	9.00×10^8	2.10×10^9	Bushveld Main Magnetite seam, South Africa	Unit	3.71×10^8	41.22	17.67
Zn-1	2.25×10^8	5.56×10^8	6.20×10^8	Krakow-Silesia Muschelkalk basin, Poland	Basin	4.00×10^7	7.19	6.45
Zn-2	2.25×10^8	5.56×10^8	6.20×10^8	Broken Hill, N.S.W., Australia	Ore zone	2.80×10^7	5.04	4.52
Ni-1	2.83×10^7	1.39×10^8	1.45×10^8	New Caledonia laterite-saprolite blanket	Area	5.00×10^7	35.97	34.48
Ni-2	2.83×10^7	1.39×10^8	1.45×10^8	Talnakh-Oktyabrskoye, Russia	Ore field	1.50×10^7	10.79	10.34
Cu-1	3.54×10^8	1.23×10^9	1.35×10^9	Copperbelt, Katanga portion, Congo Republic	Ore belt	1.25×10^8	10.16	9.26
Cu-2	3.54×10^8	1.23×10^9	1.35×10^9	El Teniente, Chile	Deposit	6.60×10^7	5.37	4.89
Co	1.15×10^6	1.20×10^7	1.50c 10^7	Copperbelt, Katanga portion, Congo Republic	Belt	1.04×10^7	86.67	69.33
Y	1.40×10^4	4.00×10^6	5.00×10^6	Tomtor, Anabar Shield, Russia	Deposit	3.00×10^6	75.00	60.00
Nb	2.72×10^5	7.00×10^7	1.10×10^8	Seis Lagoas, Brazil	Deposit	4.89×10^7	69.86	44.45
Ga	1.10×10^3	6.50×10^3	1.10×10^5	Brockman, Western Australia, Australia	Deposit	6.43×10^2	9.89	0.6
Pb-1	1.70×10^8	3.24×10^8	3.38×10^8	Viburnum Trend, S.E. Missouri, U.S.A.	Ore zone	4.80×10^7	14.81	14.20
Pb-2	1.70×10^8	3.24×10^8	3.38×10^8	Broken Hill, N.S.W., Australia	Ore zone	2.60×10^7	8.02	7.69
Th	1.30×10^4	1.20×10^6	1.62×10^6	Araxa, Brazil	Deposit	1.16×10^6	96.67	71.60
Be	1.28×10^4	7.13×10^5	8.16×10^5	Strange Lake, Labrador, Canada	Deposit	1.51×10^4	2.12	1.85
Sn-1	1.25×10^7	2.45×10^7	2.60×10^7	Kinta Valley placers, Ipoh, Malaysia	Area	3.10×10^6	12.65	11.92
Sn-2	1.25×10^7	2.45×10^7	2.60×10^7	Dachang, Jiangxi, China	Ore field	1.65×10^6	6.73	6.35
As	3.32×10^6	7.00×10^6	2.10×10^7	Rio Tinto, Spain	Ore field	4.50×10^6	64.29	21.43
U	1.86×10^6	6.70×10^6	3.20×10^7	Olympic Dam, South Australia	Deposit	1.20×10^6	17.91	3.75
Ge	1.10×10^3	6.50×10^3	1.10×10^5	Brockman, Western Australia	Deposit	6.43×10^2	9.89	0.6
Ta	4.70×10^3	1.80×10^5	4.00×10^5	Ghurayyah, Saudi Arabia	Deposit	9.33×10^4	51.83	23.33
Mo	2.43×10^6	1.45×10^7	2.84×10^7	Climax, Colorado, U.S.A.	Deposit	2.18×10^6	15.03	7.68
W	5.00×10^5	3.90×10^6	4.70×10^6	Verkhnye Qairakty, Kazakhstan	Deposit	8.80×10^5	22.56	18.72
Tl	3.10×10^2	1.20×10^4	1.70×10^4	Meggen, Germany	Deposit	9.60×10^3	80.00	56.47
Sb	2.49×10^6	7.10×10^6	7.50×10^6	Xikuangshan, Hunan, China	Ore Field	2.11×10^6	29.72	28.13
Se	5.66×10^4	3.50×10^5	7.50×10^5	Rio Tinto, Spain	Ore Field	2.25×10^5	64.35	30.00
Cd	7.44×10^5	1.75×10^6	2.20×10^6	Tsumeb, Namibia	Deposit	1.08×10^4	0.62	0.49
Bi	1.67×10^5	5.10×10^5	6.00×10^5	Shizhouyuan, Hunan, China	Deposit	2.30×10^5	44.23	38.33
Ag-1	9.47×10^5	1.28×10^6	1.37×10^6	Lubin Kupferschiefer district, Poland	District	1.70×10^5	13.32	12.44
Ag-2	9.47×10^5	1.28×10^6	1.37×10^6	Potosi (Cerro Rico), Bolivia	Deposit	7.00×10^4	5.49	5.12
In	2.80×10^3	7.40×10^3	1.20×10^4	Mount Pleasant, New Brunswick, Canada	Ore field	1.00×10^3	13.51	8.33
Hg	4.13×10^5	6.53×10^5	9.80×10^5	Almaden, Spain	Deposit	2.80×10^5	42.88	28.57
PGE	7.16×10^3	9.08×10^4	1.03×10^5	Merensky Reef, Bushveld, South Africa	Unit	4.20×10^4	46.26	40.78
Te	4.90×10^3	3.30×10^4	4.20×10^4	Cripple Creek, Colorado, U.S.A.	Ore field	1.00×10^3	3.03	2.38
Au-1	9.95×10^4	1.45×10^5	1.77×10^5	Central Rand Group, Witwatersrand, South Africa	Basin	6.30×10^4	43.40	35.60
Au-2	9.95×10^4	1.45×10^5	1.77×10^5	Welkom goldfield, Witwatersrand, South Africa	Ore field	1.53×10^4	10.55	8.64
Au-3	9.95×10^4	1.45×10^5	1.77×10^5	Welkom basal reef, Witwatersrand, South Africa	Deposit	6.50×10^3	4.48	3.67

Metals are arranged by decreasing clarke values; most ore metals are represented by a single giant locality except for Ag, Au, Cu, Pb, Ni, Sn, and Zn, where two largest genetically contrasting giant accumulations are shown

[1] Total recorded global production to 1992, compiled by S.M. Laznicka from Minerals Yearbook; gaps filled by extrapolation

[2,3] Compiled sums of global past production of ore metals plus remaining or new reserves and some resources of delineated deposits, with several calculated metal contents of geologic bodies such as the Bushveld metalliferous layers, and calculated contents of some unrecovered trace and associated metals in ores mined for other elements; because of incompleteness of the international metal endowment data the global endowment in this table is shown by a range of values between the minimum endowment (col. 3) and maximum endowment (col. 4)

[4] Ore metal content in each giant ore deposit/district

[5,6] The share of the cumulative content of metals stored in giant deposits is shown as related to both endowment limits (cols. 8 and 9)

TABLE 5. The Largest Accumulations of the Ore Metals

	Largest deposit/district[1]	Metal content (t)[2]	Tonnage accumulation index (t)[3]	Grade (ppm)	Clarke of concentration	Number of giants[4]	Metal content in all giants[5]
Al	Boke-Gaoual, Guinea	3.88×10^9	4.84×10^{10}	2.65×10^5	3.31	0	0
Fe	Alegria, Brazil	6.20×10^{10}	1.44×10^{12}	4.80×10^5	11.2	11	2.51×10^{13}
Ti	Bushveld main magnetitite seam, South Africa	2.88×10^9	7.20×10^{11}	7.20×10^4	18.0	1	9.50×10^{9} [6]
Mn	Kalahari-Mamatwan, South Africa	4.19×10^9	5.82×10^{12}	3.13×10^5	435	9	7.44×10^9
Zr	Lovozero eudialyte lujavrite unit, Russia	2.10×10^8	1.05×10^{12}	1.00×10^4	50	3	4.35×10^8
REE	Tomtor, Anabar Shield, Russia	4.00×10^7	2.67×10^{11}	8.00×10^4	533	5	9.80×10^7
Cr	Bushveld chromitite seams, South Africa	3.47×10^9	2.67×10^{13}	2.80×10^5	2,150	3	4.18×10^9
V	Bushveld main magnetitite seam, S. Africa	3.71×10^8	3.71×10^{12}	9.00×10^3	90	2	2.06×10^9
Zn-1	Krakow-Silesia Muschelkalk basin, Poland	4.00×10^7	6.15×10^{11}	4.00×10^4	615	21	3.15×10^8
Zn-2	Broken Hill, N.S.W., Australia	2.80×10^7	4.31×10^{11}	1.20×10^5	1,850	21	3.15×10^8
Ni-1	New Caledonia laterite-saprolite blanket	5.00×10^7	9.09×10^{11}	2.75×10^4	500	8	1.21×10^8
Ni-2	Talnakh-Oktyabrskoye, Russia	1.50×10^7	2.73×10^{11}	2.70×10^4	491	8	1.21×10^8
Cu-1	Copperbelt, Katanga portion, Congo Republic	1.25×10^8	5.00×10^{12}	4.25×10^4	1,700	103	1.23×10^9
Cu-2	El Teniente, Chile	6.60×10^7	2.60×10^{12}	1.31×10^4	524	103	1.23×10^9
Co	Copperbelt, Katanga portion, Congo Republic	1.04×10^7	4.31×10^{11}	2.30×10^3	96	3	1.20×10^7
Y	Tomtor, Anabar Shield, Russia	3.00×10^6	1.25×10^{11}	6.00×10^3	250	1	3.00×10^6
Nb	Seis Lagoas, Brazil	4.89×10^7	2.57×10^{12}	1.70×10^4	895	6	1.04×10^8
Ga	Brockman, Western Australia, Australia	6.43×10^2	4.29×10^7	1.50×10^2	10.0	0	0
Pb-1	Viburnum Trend, S.E. Missouri, U.S.A.	4.80×10^7	3.20×10^{12}	4.00×10^4	4,000	55	3.02×10^8
Pb-2	Broken Hill, N.S.W., Australia	2.60×10^7	1.73×10^{12}	1.13×10^5	7,530	55	3.02×10^8
Th	Araxa, Brazil	1.16×10^6	1.36×10^{11}	6.20×10^2	73	1	1.16×10^6
Be	Strange Lake, Labrador, Canada	1.51×10^4	6.28×10^9	3.00×10^2	125	0	0
Sn-1	Kinta Valley placers, Ipoh, Malaysia	3.10×10^6	1.35×10^{12}	5.00×10^2	217	22	$2.38c10^7$
Sn-2	Dachang, Jiangxi, China	1.65×10^6	7.17×10^{11}	1.30×10^4	5,650	22	2.38×10^7
As	Rio Tinto, Spain	4.60×10^6	2.65×10^{12}	6.00×10^3	3,530	9	8.65×10^6
U	Olympic Dam, South Australia	1.20×10^6	7.06×10^{11}	5.40×10^2	318	9	3.45×10^6
Ge	Tsumeb, Namibia	2.16×10^3	1.54×10^9	5.00×10^1	36	0	0
Ta	Ghurayyah, Saudi Arabia	9.33×10^4	8.48×10^{10}	2.12×10^2	193	0	0
Mo	Climax , Colorado, U.S.A.	2.18×10^6	1.98×10^{12}	2.40×10^3	2,180	41	2.74×10^7
W	Verkhnye Qairakty, Kazakhstan	8.80×10^5	8.80×10^{11}	1.02×10^3	1,020	12	3.63×10^6
Tl	Meggen, Germany	9.60×10^3	2.40×10^6	2.40×10^2	600	0	0
Sb	Xikuangshan, Hunan, China	2.11×10^6	7.02×10^{12}	2.90×10^4	96,700	24	6.97×10^6
Se	Rio Tinto, Spain	2.25×10^5	1.88×10^{12}	3.00×10^2	2,500	1	2.25×10^5
Cd	Tsumeb, Namibia	1.08×10^4	1.08×10^{11}	4.00×10^2	4,000	1	1.08×10^4
Bi	Shizhouyuan, Hunan, China	2.30×10^5	2.71×10^{12}	1.00×10^3	11,800	5	5.20×10^5
Ag-1	Lubin Kupferschiefer district, Poland	1.70×10^5	2.43×10^{12}	4.00×10^1	571	43	8.59×10^5
Ag-2	Potosi (Cerro Rico), Bolivia	7.00×10^4	1.00×10^{12}	3.00×10^2	4,290	43	8.59×10^5
In	Mount Pleasant, New Brunswick, Canada	1.00×10^3	2.00×10^{10}	1.50×10^2	3,000	0	0
Hg	Almaden, Spain	2.80×10^5	7.00×10^{12}	1.50×10^4	375,000	19	9.50×10^5
PGE	Merensky Reef, Bushveld, South Africa	4.20×10^4	3.23×10^{12}	6.00	462	7	9.08×10^4
Te	Cripple Creek, Colorado, U.S.A.	1.00×10^3	2.00×10^{11}	8.50×10^1	17,000	1	1.00×10^3
Au-1	Central Rand Group, Witwatersrand, S. Africa	6.30×10^4	2.52×10^{13}	6.50	2,600	99	9.72×10^5
Au-2	Welkom gold field, Witwatersrand, S. Africa	1.53×10^4	6.12×10^{12}	1.16×10^1	4,640	99	9.72×10^5
Au-3	Welkom basal reef, Witwatersrand, S. Africa	6.60×10^3	2.60×10^{12}	1.16×10^1	4,640	99	9.72×10^5

[1] Localities as in Table 4, metals are arranged by decreasing clarke values; Most metals are represented by a single oversize locality except for Al, Au, Cu, Pb, Ni, Sn, and Zn where two largest genetically contrasting metal accumulations are shown

[2] Published, calculated, or extrapolated geologic reserves

[3] Tonnage accumulation index in tons of crustal equivalent

[4] Number of giant and supergiant deposits of the world

[5] Cumulative ore metal tonnage in all giant and supergiant deposits

[6] Includes Ti in all Bushveld Ti-magnetite seams to depth of 1.5 km

Based on the quantitative criteria outlined above, there are presently 486 entries that qualify as giant and 61 entries that qualify as supergiant in the GIANTDEP database. The entries (one entry per metal/locality) equate into 446 localities. As expected, the absolute magnitude of metal accumulation generally increases with the increasing geochemical abundance of elements (McKelvey, 1960; Erickson, 1973), but the increase is not systematic. This is due to several reasons, some of which are entirely extraneous to geology, whereas the others are probably the consequence of the geochemical behavior of elements in the various rock- and ore-forming systems.

One obvious extraneous factor impacting the frequency of giant deposits of several metals is the differences in price and market demand, which do not closely correlate with the crustal abundances of elements. The high-demand metals such as Fe, Cu, Pb, and Au have been eagerly sought and exploited for centuries. Hence, every newly found deposit usually goes into production within a few years and the inventory of localities increases. The limited-demand metals such as Zr, Nb, and REE are produced and supplied by several specialty producers serving generally captive markets. The already known but substantially unexploited resources of

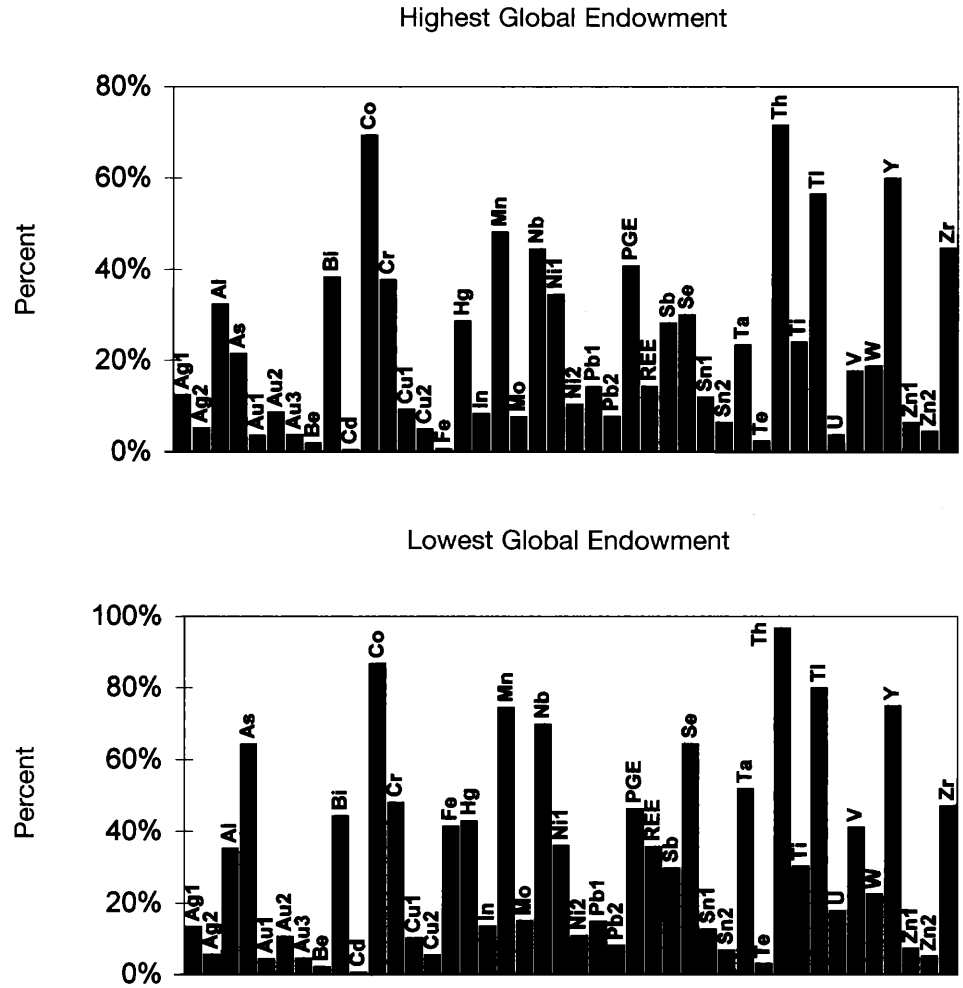

FIG. 1. Share of the total world metal reserves by the largest giant deposits/districts of each metal, based on data in Table 4. Because exact values of the global reserves of ore metals that reside in deposits of any size are not available, they are believed to reside between the highest (top chart) and lowest (bottom chart) tonnage limits. These limits then determine the share of the industrial metals stored in giant accumulations.

Zr, Nb, and REE are sufficient for several hundred years at the present rate of consumption, so there is little incentive for vigorous exploration. Therefore, the inventory of known deposits increases slowly if at all. The inventory of deposits of the nil-demand metals such as thorium is stagnant and fragmentary. The examples of Th accumulations included here, as in the U conglomerates of Elliot Lake, Ontario, and the Nb carbonatite at Araxa, Brazil, are calculated Th contents in ore but the metal is not recovered at present. Certain inexpensive metals are grossly undervalued in relation to their geochemical scarcity. The most striking example is antimony, with a clarke value of only 3.0×10^{-1}, that sells for about US$4.0/k, in contrast with the more abundant Ni, with a clarke value of 5.5×10^{1} , that normally sells for about US$7.0/k. One reason for the low price of antimony is that it forms highly concentrated deposits that are cheap to mine and process. Antimony and mercury deposits, especially the three supergiants Almaden (Hg) Spain, Idrija (Hg) Slovenija, and Xikuangshan (Sb) China, have achieved the greatest magnitudes of the relative metal concentration and accumulation ever recorded (Fig. 3).

Table 5 (col. 2 from the right) gives the number of giant and supergiant deposits of each metal included in the GIANTDEP database. The number of giants sequence, arranged by the decreasing number of entries, is as follows (the number of entries from Table 5 is in parentheses): Cu (103), Au (99), Pb (55), Ag (43), Mo (41), Sb (24), Sn (22), Zn (21), Hg (19), W (12), Fe (11), As (9), U (9), Mn (9), Ni (8), PGE (7), Nb (6), REE (5), Bi (5), Co (3), Cr (3), Zr (3), V (2), Cd (1), Th (1), Ti (1), and Y (1). There are no giant deposits of the following elements: Al, Be, Ga, Ge, In, Sc, Ta, and Tl, for a variety of reasons. For example, aluminum is the most abundant metal in the crust with a clarke value of 8×10^{4}, not counting Si. The threshold for the giant magnitude of Al deposits is 8 bt of contained Al. No deposit or area of bauxite, presently the only viable Al ore, approaches such an endowment. If anorthosite becomes an industrial aluminum ore, many anorthosite massifs will become giant deposits. Ta, as geochemically abundant as Mo (1.1 ppm), and Ga and Sc, as geochemically abundant as Pb (15 ppm), tend to remain dispersed and substitute for other elements in the lattices of various minerals. Ta forms low concentrated accumulations in the highest fractionated

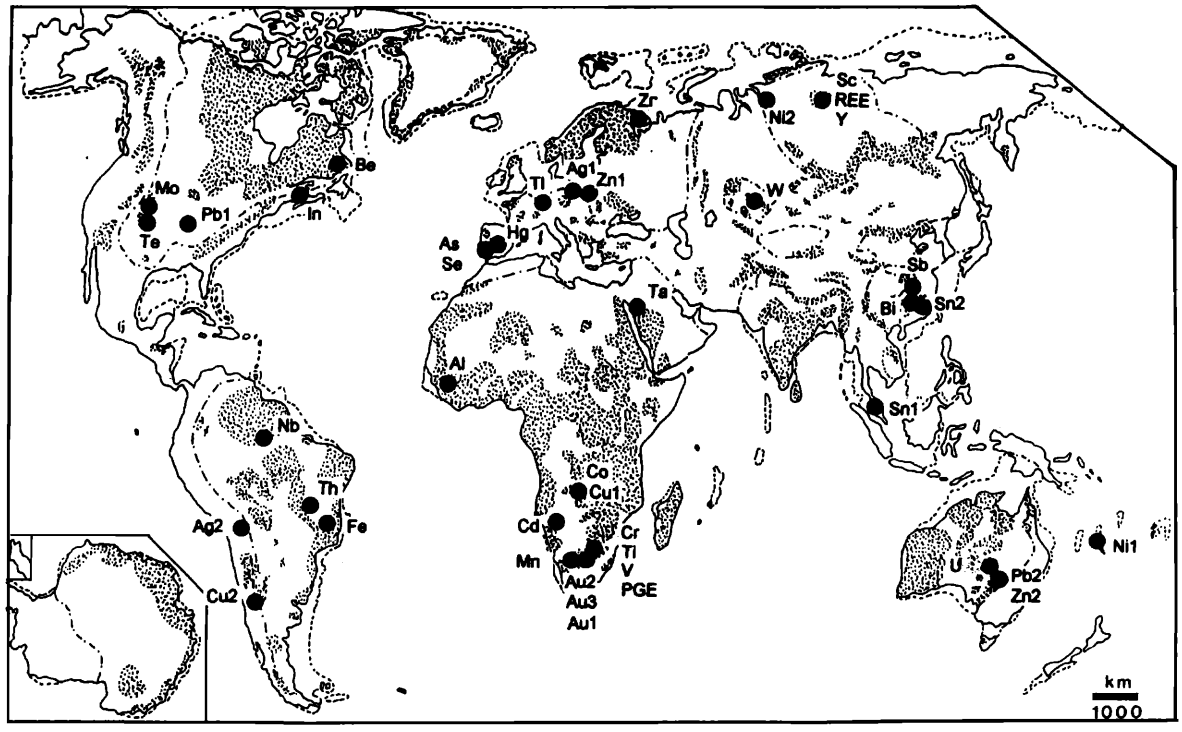

FIG. 2. The largest accumulations of each ore metal. A single locality is shown for most metals, although two localities of contrasting type are shown for Ag, Cu, Ni, Pb, Sn, and Zn and three localities are of gold. Stippled areas show Precambrian outcrop, dash-dot lines indicate limit of Precambrian in subsurface, and broad continental shelves are outlined by a dashed line.

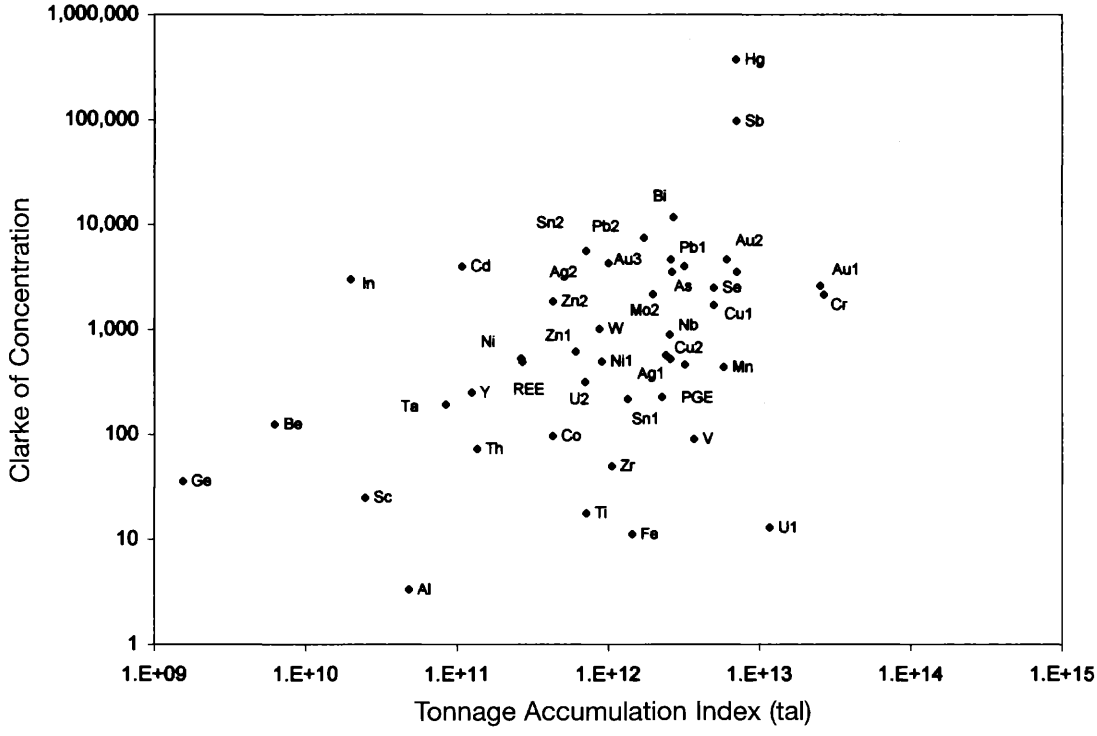

FIG. 3. Plot of the clarke of concentration (vertical axis) against the tonnage-accumulation index (horizontal axis) of the largest ore accumulations of each metal based on data in Table 5. Ag, Cu, Ni, Pb, Sn, and Zn are each represented by two localities of a contrasting type.

granitic and alkaline systems, but Ge and Sc rarely form minerals of their own. Gallite ($CuGaS_2$) and thortveitite [$(Sc,Y)_2Si_2O_7$] are mineralogical rarities known from few localities. Despite the rarity of Ga and Sc, the market for these elements is extremely limited. Tl and In are rare to moderately rare metals that accumulate in sulfide deposits and are recovered from electrolytic residuum to supply a very limited market (Carlin, 1985; Plunkert, 1985).

Giant Metal Deposits Quantified by Origin

There is no perfect geologic classification of ore deposits that would accommodate every recorded mineralized locality without controversy or alternative placement. There are many reasons for this, of which transitionality, interactive and multistage origin, and conceptual uncertainty are the most important ones. Only a portion of the giant metal accumulations in the GIANTDEP file fit reasonably well into the genetic, environmental, or associational classes distinguished in textbooks (Lindgren, 1933; Schneiderhöhn, 1955; Routhier, 1963; Smirnov, 1976; Guilbert and Park, 1986; Sawkins, 1990; Pohl, 1992) and not all correspond to a distinct type or model, such as one of the U.S. Geological Survey mineral deposit models (Cox and Singer, 1986). The most commonly represented traditional genetic groups or ore types are given in Table 6. A new organization of giant ore deposits, into which every entry in GIANTDEP can fit, has been prepared for this study. It is explained below and the results are given in Table 7 and Figure 4.

The bulk of the giant accumulations and most lesser size deposits of the base, rare, and precious metals precipitated from hydrous fluids (Fyfe et al., 1978). The hydrous regimes in the present classification have been subdivided into two families: (1) surface waters (where water is implied as an agent of sedimentogenesis and of chemical weathering in the sedimentary and weathering-related categories), and subsurface aqueous fluids (considered as a part of the low-temperature rock diagenesis and ground-water circulation credited with formation of metal accumulations in the categories designated as "aqua"); and (2) hydrothermal fluids exsolved from magmas and/or heated by magmatic and metamorphic (geothermal) systems. Hydrothermal deposits ("hydro") make up the largest genetic family, subdivided into several lesser categories by increasing temperature (hot spring, epithermal, mesothermal), special affiliation (e.g., a hydrothermal phase of alkaline intrusions), and transitionality (hydrothermal-sedimentary, i.e., representing ores precipitated from in depth-generated hydrothermal fluids discharged on the sea floor as in the sedimentary exhalative type; hydrothermal volcanic-sedimentary as in the volcanics-associated massive sulfides).

TABLE 6. Conventional Types of Giant and Supergiant Ore Metal Accumulations

Ore type	Number of giant and supergiant deposits/districts
Epithermal Ag	3
Epithermal Au-Ag	13
Epithermal Au	7
Epithermal Pb-Zn-Ag	4
Scheelite skarn	4
Porphyry Cu-Au	6
Porphyry Cu-Mo	90
Porphyry (stockwork) Mo	17
Sedex Zn-Pb-Ag	23
Volcanics-associated massive sulfides (various metals)	22
Broken Hill-type (high-grade metamorphic) Zn-Pb-Ag	12
Placer Au	7

Hydrothermal ore deposits are commonly associated with magmatic systems (Burnham, 1979; Brimhall and Crerar, 1989; Candela, 1989). Barton (1996) recognized three, presumably transitional, categories of ore-forming hydrothermal fluids in respect to magmas: (1) those where magmatic fluids and heat are essential, (2) those where magmatic heat is essential and magmatic fluids problematic, and (3) those where the magmatic link is problematic. Hydrothermal deposits that precipitated from (1) and (2) fluids show spatial and temporal correlation with intrusions, a feature absent in (3). Ores that precipitated from magmatic fluids (1), moreover, show a repetitive association between magmatic families and characteristic metals or metals sets (Abdullayev, 1964; Urabe, 1985; Keith, 1986; Shaw and Guilbert, 1990; Keith et al., 1991; Blevin and Chappell, 1992). This feature is well developed among the giant and supergiant ore deposits and 182 entries show a good magma/metals correlation (Table 8; Fig. 5).

In the number of database entries, the most prolific igneous parent to giant and supergiant accumulations is the calc-alkaline metaluminous granodiorite-quartz monzonite association of subducted continental margins. Keith and Swan (1996) reviewed in detail the great porphyry copper cluster in Arizona, Sonora, and adjacent parts of New Mexico that contains 187 known porphyry Cu-Mo districts of Mesozoic to mid-Cainozoic age, 12 of which are of giant magnitude. They characterize the Cu-Mo orebodies as being in and marginal to hornblende-biotite granodiorite stocks, members of the metaluminous, calc-alkaline magma series.

Hydrothermal metal accumulations in which the magmatic link is problematic (category 3 of Barton, 1996) include the metamorphic-hydrothermal and orogenic lode gold deposits that are especially common in accretionary wedges (e.g., Mother Lode, California; Juneau district, Alaska; Victoria Goldfields, Australia; Goldfarb et al., 1993) and close to major deformation zones in Archean greenstone complexes (Eastern Goldfields, Australia; Abitibi subprovince, Canada; Groves et al., 1997; Colvine, 1989). Gold is thought to have precipitated from hydrous fluids derived by syntectonic orogenic heating, pressure filtering, and deep dehydration. The native copper and/or chalcocite-mineralized meta-basalt flow tops of the Keweenawan Supergroup, Michigan, are interpreted as products of precipitation of copper leached from the volcanic pile at depth by fluids released during metamorphic dehydration and deposited at the greenschist-prehnite-pumpellyite metamorphic interface (Bornhorst et al., 1988). In the present study, these flow tops are placed into the hydrothermal-metamorphic category.

The still enigmatic, low-temperature cinnabar deposits in sedimentary rocks or ophiolitic melange associated with faults and folds, which, because of the extremely low Hg crustal clarke, have a strong presence among the giant deposits (e.g., Almaden, Spain; Idrija, Slovenija; New Almaden, California)

TABLE 7. Genetic Classes of Giant and Supergiant Deposits

Genetic class	Metal	No.of giant and supergiant deposits	Cumulative tonnage of metal
Hydrothermal-sedimentary	Au	1	3.11×10^2
Hydrothermal volcanic/sedimentary	Ag	3	4.57×10^4
Hydrothermal volcanic/sedimentary	As	1	4.50×10^6
Hydrothermal volcanic/sedimentary	Au	3	1.95×10^3
Hydrothermal volcanic/sedimentary	Cu	5	1.56×10^7
Hydrothermal volcanic/sedimentary	Fe	1	1.20×10^{10}
Hydrothermal volcanic/sedimentary	Pb	7	3.90×10^7
Hydrothermal volcanic/sedimentary	Zn	3	5.63×10^7
Hydrothermal volcanic/sedimentary	Sb	1	2.18×10^5
Magmatic-alkaline	Nb	2	1.50×10^7
Magmatic-alkaline	REE	2	7.50×10^6
Magmatic-alkaline	Zr	2	2.60×10^8
Magmatic-carbonatite	Cu	1	1.10×10^7
Magmatic-carbonatite	Nb	3	8.67×10^7
Magmatic-carbonatite	REE	2	5.45×10^7
Magmatic-carbonatite	Th	1	1.16×10^6
Magmatic-carbonatite	Y	1	3.00×10^6
Magmatic-mafic	Cu	3	7.31×10^7
Magmatic-mafic	Fe	1	6.60×10^{10}
Magmatic-mafic	Ni	4	5.17×10^7
Magmatic-mafic	PGE	6	8.91×10^6
Magmatic-mafic	Ti	1	2.88×10^9
Magmatic-mafic	V	1	3.71×10^8
Magmatic-pegmatitic	Sn	1	5.00×10^5
Magmatic-ultramafic	Cr	3	4.18×10^9
Magmatic-ultramafic	Cu	1	3.42×10^6
Magmatic-ultramafic	Ni	1	5.60×10^6
Magmatic-ultramafic	PGE	1	1.68×10^3
Metamorphicorphic-hydrothermal	Cu	3	1.67×10^7
Sedimentary-authigenic	Mo	1	3.20×10^5
Sedimentary-authigenic	U	1	3.00×10^5
Sedimentary-chemical	Fe	7	1.09×10^{11}
Sedimentary-chemical	Mn	8	7.16×10^9
Sedimentary-chemical-(metamorphic)	Fe	2	6.41×10^{10}
Sedimentary-clastic	Au	17	5.23×10^4
Sedimentary-clastic	U	1	4.84×10^4
Sedimentary-evaporitic	Li	2	9.10×10^6
Volcanic-diagenetic	Cu	1	4.50×10^6
Volcanic-diagenetic	Li	1	2.25×10^6
Weathering-residual/reworked	Sn	8	1.24×10^8
Weathering-residual	Co	1	2.50×10^6
Weathering-residual	Mn	1	2.75×10^8
Weathering-residual	Ni	3	6.33×10^7
Weathering-sulfide	Au	1	3.25×10^2
Aqua (subhydrothermal)	Hg	12	7.92×10^5
Aqua (subhydrothermal)	Pb	1	3.20×10^6
Aqua (subhydrothermal)	Sb	1	1.75×10^5
Aqua ? (subhydrothermal)	Cu	1	2.64×10^6
Aqua-carbonate (subhydrothermal)	Hg	4	1.06×10^5
Aqua-carbonate (subhydrothermal)	Pb	9	8.18×10^7
Aqua-carbonate (subhydrothermal)	Zn	4	6.27×10^7
Aqua-redo x (subhydrothermal)	Ag	2	1.82×10^5
Aqua-redo x (subhydrothermal)	Co	2	9.51×10^6
Aqua-redo x (subhydrothermal)	Cu	19	3.56×10^8
Aqua-redo x (subhydrothermal)	Pb	1	2.60×10^6
Aqua-redo x (subhydrothermal)	U	2	6.29×10^5
Aqua-redo x ? (subhydrothermal)	Cu	1	3.05×10^6
Aqua-unconformity	U	3	5.35×10^5
High-grade metamorphic	Ag	3	7.42×10^4
High-grade metamorphic	Cu	1	2.50×10^6
High-grade metamorphic	Pb	5	4.12×10^7
High-grade metamorphic	Zn	4	5.88×10^7
High-grade metamorphic	Zr	1	2.50×10^7
Hydrothermal-alkaline	Nb	1	2.00×10^6
Hydrothermal-alkaline	REE	1	3.60×10^7
Hydrothermal-brine	Ag	1	1.09×10^4
Hydro-epithermal	Ag	12	2.99×10^5
Hydro-epithermal	As	1	5.44×10^5
Hydro-epithermal	Au	16	7.14×10^3
Hydro-epithermal	Pb	3	1.23×10^7
Hydrothermal-hot spring	Hg	2	2.08×10^4
Hydro-mesothermal	Ag	16	1.90×10^5
Hydro-mesothermal	As	7	3.61×10^6
Hydro-mesothermal	Au	61	3.52×10^4
Hydro-mesothermal	Bi	5	5.20×10^5
Hydro-mesothermal	Cd	1	1.08×10^4
Hydro-mesothermal	Cu	67	7.34×10^8
Hydro-mesothermal	Hg	1	3.15×10^4
Hydro-mesothermal	Mo	39	2.69×10^7
Hydro-mesothermal	Pb	19	5.94×10^7
Hydro-mesothermal	Sb	22	6.58×10^6
Hydro-mesothermal	Sn	13	1.09×10^7
Hydro-mesothermal	Te	3	3.39×10^3
Hydro-mesothermal	U	2	1.50×10^6
Hydro-mesothermal	W	12	3.63×10^6
Hydro-mesothermal	Zn	3	3.00×10^7
Hydrothermal-sedimentary	Ag	6	5.71×10^4
Hydrothermal-sedimentary	Pb	10	6.23×10^7
Hydrothermal-sedimentary	Zn	7	1.07×10^8

have hitherto been treated as hot-spring, telethermal, epithermal, or exhalative metalizations. This is probably true for the deposits situated in terranes with synchronous volcanism or magma-driven geothermal circulation, as in the Clear Lake region of California (the Sulfur Bank Hg deposit; Rytuba, 1993), in the McDermitt caldera, Nevada and Oregon (Rytuba and Glanzman, 1979), and partly in the Monte Amiata district of Tuscany (Dessau, 1977), but it does not apply to the three giant and supergiant Hg accumulations mentioned above. Low-temperature remobilization of cinnabar or native mercury into dilations controlled by tight folds (Almaden; Saupe, 1990; Jébrak and Hernandez, 1995) or major fault zones (Idrija, Khaidarkan; Bercé, 1958; Nikiforov, 1976) would place these deposits into the aqua Hg category. The New Almaden Hg deposit in the Franciscan terrane of California (Bailey and Everhart, 1964) has been interpreted by Rytuba (1996) as a product of near-surface precipitation from low-temperature, high CO_2 fluids derived from connate waters above a thermal anomaly related to a slab window, i.e., an epithermal environment, essentially the same as all other California Coast Range Hg deposits (Peabody and Einaudi, 1992).

Orthomagmatic and pegmatitic metal accumulations of Cr, PGE, Ni, Fe-Ti-V, Li-Sn-Ta, Nb-REE, and Zr have a particularly strong association with distinct magmatic families (Schneiderhöhn, 1941; Sørensen, 1974; Naldrett, 1989; Wilson, 1989). When the frequency of occurrence of giant metal accumulations is contrasted with the abundance of parent intrusions of distinct petrochemistry and origin, the most prolific single magmatic family is carbonatite. Carbonatite forms rare isolated occurrences but most frequently it participates in a joint nephelinite-carbonatite association (especially

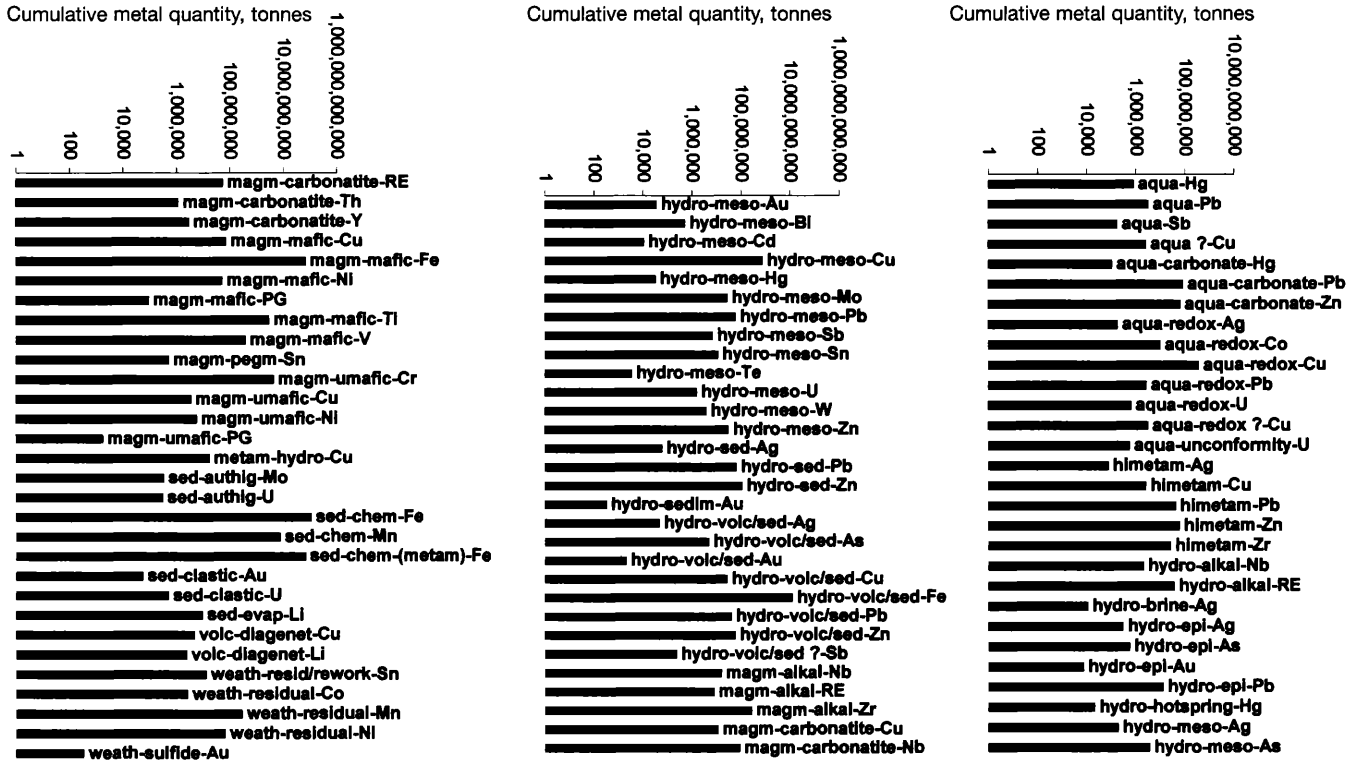

FIG. 4. Cumulative quantities of ore metals in giant and supergiant ore deposits in the various genetic classes listed in Table 7.

TABLE 8. Giant and Supergiant Metal Accumulations Organized by Magmatic Families with which they are Genetically Associated

Number in Figure 5	Magmatic family, metal	Cumulative metal content	No. of deposits
1	Alkaline agpaitic, Nb	15×10^7	2
2	Alkaline agpaitic, REE	7.5×10^6	2
3	Alkaline agpaitic, Zr	2.6×10^8	2
4	Alkaline-ultramafic, Cu	11.05×10^7	1
5	Carbonatite, Nb	8.76×10^7	3
6	Carbonatite, REE	5.446×10^7	2
7	Carbonatite, Th	1.16×10^6	1
8	Carbonatite, Y	3.0×10^6	1
9	Diorite-monzonite, Ag	1.4×10^4	1
10	Diorite-monzonite, Au	2.1×10^3	2
11	Diorite-monzonite, Cu	3.72×10^7	4
12	Fe tholeiite, Cr	3.47×10^9	1
13	Fe tholeiite, Cu	7.313×10^7	3
14	Fe tholeiite, Fe	6.6×10^{10}	1
15	Fe tholeiite, Ni	5.172×10^7	4
16	Fe tholeiite, PGE	8.9125×10^4	6
17	Fe tholeiite, Ti	2.88×10^9	1
18	Fe tholeiite, V	3.71×10^8	1
19	K granite, Ag	2.0×10^4	1
20	K granite, Bi	3.0×10^4	1
21	K granite, Sn	2.23×10^7	19
22	K granite, W	2.715×10^5	2
23	Metaluminous granodiorite-qz monzonite, Ag	31.23×10^4	3
24	Metaluminous granodiorite-qz monzonite, Au	3.343×10^3	6
25	Metaluminous granodiorite-qz monzonite, Cu	6.13×10^8	58
26	Metaluminous granodiorite-qz monzonite, Mo	2.083×10^7	30
27	Metaluminous granodiorite-qz monzonite, W	2.7×10^5	1
28	Metaluminous granite, Bi	4.68×10^5	3
29	Metaluminous granite, Mo	6.065×10^6	7
30	Metaluminous granite, Sn	4.2×10^5	1
31	Metaluminous granite, Te	8.8×10^2	1
32	Metaluminous granite, W	1.48×10^6	2
33	Mid-ocean ridge basalt, Cr	3.5×10^7	1
34	Peralkalkaline granite, Li	2.25×10^6	1
35	Peralkalkaline granite, Sn	5.5×10^5	1
36	Peraluminous pegmatite, Sn	5.0×10^5	1
37	Peridotite, Cr	6.82×10^8	1
38	Peridotite, Cu	3.417×10^6	1
39	Peridotite, Ni	5.6×10^6	1
40	Peridotite, PGE	1.68×10^3	1
41	Syenite-trachyte, Au	7.55×10^2	1

n = 128 entries

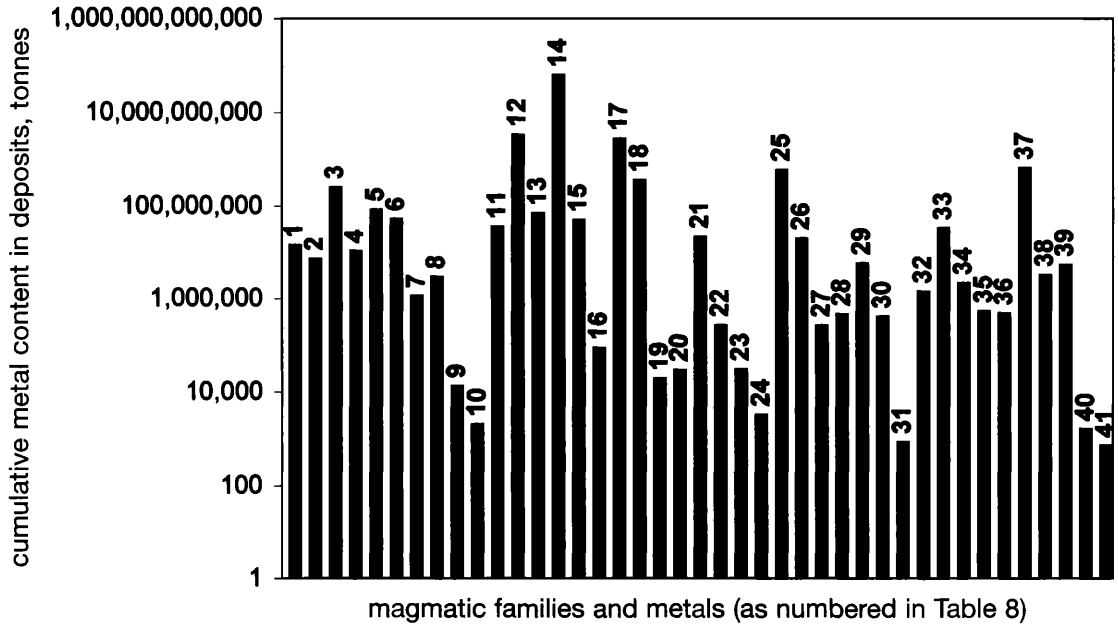

FIG. 5. Giant metal deposits and districts organized by magmatic families with which they are genetically associated. The numbered magmatic families are explained in Table 8. n = 182 entries.

at high crustal levels; Le Bas, 1987). It also appears as a frequent extreme fractionate in agpaitic suites dominated by nepheline syenitic rocks, as well as in alkaline-ultramafic suites in association with pyroxenite. Presently there are about 330 carbonatite occurrences recorded worldwide (Wooley, 1989), to which should be addedd the less well known occurrences in the former U.S.S.R., Mongolia, and China (Samoilov, 1984), for a total of about 350. Five of the carbonatites host giant or supergiant Nb, REE, Th, and Cu deposits, and an additional 11 carbonatites host large deposits of these metals. This corresponds to 1.4 and 3.1 percent of the entire global inventory of carbonatites, respectively. As several carbonatites are multiple giants (they accommodate more than one ore metal in exceptional quantities, e.g., Araxa, Brazil, and Tomtor, Siberia, jointly host giant Nb, REE, and Th accumulations), the giant and large accumulations of ore in carbonatites account for 21 entries in the GIANTDEP database. These statistics suggest that any discovery of a new carbonatite has about a 4.5 percent chance to become a giant or a large metal accumulation. No other rock association has such a high chance of hosting a giant or large metal deposit.

Alkaline rocks are substantially more abundant in the lithosphere than carbonatites, yet they are rare rocks that are credited with occupying no more than 0.2 to 0.3 percent of the continents by area (Sørensen, 1974). Nine alkaline complexes without carbonatites and 25 complexes with carbonatites are associated with six giant and 12 large deposits in the GIANTDEP database as some localities are multimetal accumulations. This represents about 2.5 percent, without carbonatites, and 7 percent, with carbonatites, of the entire giant-supergiant population of metallic deposits. Alkaline- and carbonatite-hosted giant metal accumulations store about 103 Mt of Nb, 72 Mt of REE, 260 Mt of Zr, 1.16 Mt of Th, and 3.2 Mt of Y in potentially mineable orebodies. Eleven Mt of Cu are accumulated in the single giant carbonatite-hosted deposit Palabora, South Africa.

Giant Metal Accumulations in Geologic Time

Have any giant deposits formed during the Quaternary? The answer is yes as indicated by the GIANTDEP database where Quaternary giants include seven gold placers, two lithium accumulations in playa lakes, 18 weathering residual deposits of Fe, Sn, Co, Ni, Mn, Au, and one Quaternary hot spring-type Hg deposit (Sulfur Bank, California; Rytuba, 1993). The presently forming or recently formed hydrothermal sulfide and oxide accumulations on the sea floor in the Red Sea Rift basin, at oceanic spreading ridges, and in the back-arc-interarc settings (Rona and Scott, 1993; Herzig and Hannington, 1995; Duckworth et al., 1998) are not sufficiently delineated and most are not large enough to be giant deposits. The vast accumulation of Mn, Co, Ni, and Cu in the ferromanganese nodules on the abyssal ocean floor has not been considered here as no industrial deposits have been outlined so far. Of several presently active metalization processes that have the potential to eventually produce a giant deposit, two will be briefly reviewed.

At Rotokawa hot springs, Taupo Volcanic Zone, New Zealand, thermal springs discharge into a shallow acid lake located in a hydrothermal explosion crater within a large rhyolitic caldera. Bedded native sulfur hosted by lacustrine muds has been mined intermittently in the past (Krupp and Seward, 1987; Sinclair, 1989). Finely divided gold associated with high concentrations of As and Sb sulfides and native sulfur precipitates from present springs and accumulates in bright yellow, green, and orange arsenic-rich muds that are interstratified with lacustrine muds. The total demonstrable gold resource in the muds is about 250 kg Au at an average grade of 1 ppm Au, but Krupp and Seward (1987) have calculated

that up to 370 t Au could have been transported into the region beneath the crater in the past 6,060 yr by a fluid saturated with 7.2 mg/kg Au at the present flow rate of 5.5 kg/sec, to possibly form a giant accumulation at a depth of several hundred meters.

Giant Au placers have been forming since Miocene time on both sides of the transpressional Alpine fault of New Zealand (Henley and Adams, 1979). A steady uplift sustains erosion of hydrothermally mineralized strata continuously brought to the surface from depth. Gold content has been possibly augmented by gold precipitation from metamorphic and geothermally heated water along faults, the formation of structural basins to accumulate detritus, and chemical mobilization of gold (Youngson and Craw, 1995). Glacial erosion may have been an additional effective mechanism to sweep a broad area of low-grade gold mineralization and to redeposit the detritus far away from the source to undergo stream reworking and gold enrichment. Similar processes contributed to gold placer formation in Alaska (Nome; Nelson and Hopkins, 1972), Yakutia, and in the Lena (Bodaibo) goldfield of Siberia (Bilibin, 1955).

Metalliferous placers, and in fact most of the recent surface or near-surface metal accumulations regardless of the size of deposits, are rarely preserved. Alluvial placers and lateritic crusts, in particular, are eroded almost as fast as they form. The pre-Quaternary ore deposits have escaped dispersal because of special events such as deep downfaulting in rifts and grabens and/or burial under lava flows or pyroclastics (the deep leads of the Victoria goldfields, especially Bendigo, under basalts; Phillips and Hughes, 1996; the fossil-enriched zones over the western United States porphyry copper deposits under young volcanics; Livingston et al., 1968). The portion of the Witwatersrand reefs that has survived erosional removal shortly after deposition was preserved by downfaulting and burial under the Klipriviersberg Group basalts (Myers et al., 1990). The Ventersdorp contact reef, a secondary placer situated at the Central Rand-Klipriviersberg unconformity (McCarthy, 1994), formed by cannibalization of the Central Rand orebodies simultaneously with the footwall dissection, removal, and reworking of the reefs.

The preservation factor strongly influences the distribution of giant deposits in geologic time and the selection of metals and ore types as shown in Tables 9 and 10 and in Figure 6. The most favorable time interval of occurrence of giant deposits is between the mid-Tertiary and late Mesozoic during which most of the high-level epithermal and porphyry deposits formed. A good correlation exists between the early Tertiary ore-forming peak in Figure 6 and the mesothermal Cu and Mo categories in Figure 4 that include porphyry Cu-Mo and stockwork Mo deposits. There is no substantial difference between the distribution of giant deposits and any lesser size ore deposits of the same metals and types in agreement with prior studies (Laznicka, 1993; Meyer, 1981). The preliminary results obtained by research in progress indicate that if the pattern of ore distribution in time as shown in Figure 6 was normalized by the typical depth of ore emplacement corrected by calculated rates of the postemplacement tectonic and epeirogenic uplift and denudation, the statistical maxima and minima in the global ore distribution would lose much of the contrast, at least through the Paleozoic. This indicates that preservation is the substantially stronger control mechanism than evolution in influencing the distribution pattern of the ancient metalizations.

Conclusions

Are giant deposits and/or the processes, settings, and conditions under which they were formed qualitatively different from smaller deposits and their formational processes with which we are generally familiar, or are giant deposits just the magnitude peaks in populations of all deposits of a given type? On a statistical basis the second alternative is clearly predominant. In addition to the explicit support given to this alternative in the literature (Laznicka, 1989, 1998b; Clark, 1993; Sillitoe, 1993; Phillips et al., 1996), giant deposits are

TABLE 9. Giant and Supergiant Metal Accumulations in Geologic Time/Number of Deposits

	Total	Ag	As	Au	Bi	Cd	Co	Cr	Cu	Fe	Hg	Li	Mn	Mo	Nb	Ni	Pb	PG	RE	Sb	Sn	Te	Th	Tl	U	V	W	Y	Zn	Zr
No date	5	1								1				3																
Q: 0-2 Ma	23	1		8			1		1		1	2				3					6									
T_2: 2-25 Ma	59	2		21					14		10	1		5			4			1	1									
T_1: 25-60 Ma	103	19	2	5					30		3		4	26			5			4	3	1							1	
Cr_2: 60-100 Ma	21	2		2					9		1			1						2							4			
Cr_1: 100-150 Ma	26			8					5	1			1	1	1		4		1				1		1		2			
J: 150-210 Ma	39	1	1	7	2				3					2	1		3		1	5	6				2		3	1		1
Tr: 210-245 Ma	14	2							5		2					1	2	1											1	
Pe: 245-290 Ma	13	1			1						1			1	1		1			3	1						2			
Cb: 290-354	37	1	3	9	1				7		1						7			3	1								3	
S-D: 354-440 Ma	28		1	5				1							1		9		2	4	1						1		2	1
Or: 440-500 Ma	8	2															2		1	1									2	
Cm: 500-550 Ma	9	1												1	1		4								1				1	
Np: 550-1000 Ma	31		1	4		1	1		14	2			1				3				2								1	
Mp: 1.0-1.6 Ga	25	3		2					6						1	1	3				1				4				3	1
Pp_2: 1.6-2.0 Ga	33	5	1	3					6	1			1			2	8	1											5	
Pp_1: 2.0-2.45 Ga	23	1		1	1			2	2	6			2			1		4							1				1	
Ar: 2.45-3.0 Ga	31	1		24					1					1				1		1						1			1	

Abbreviations: Ar = Archean; Cb = Carboniferous; Cm = Cambrian; Cr_1 = lower Cretaceous; Cr_2 = upper Cretaceous; J = Jurassic; Mp = Mesoproterozoic; Np = Neoproterozoic; Or = Ordovician; Pe = Permian; PG = PGE; Pp_1 = lower Paleoproterozoic; Pp_2 = upper Paleoproterozoic; Q = Quaternary; RE = REE; S-D = Silurian, Devonian; T_1 = lower Tertiary; T_2 = upper Tertiary; Tr = Triassic

TABLE 10. Giant and Supergiant Metal Accumulations in Geological Time/Cumulative Tonnage

	Ag	As	Au	Bi	Cd	Co	Cr	Cu	Fe
No date	2.00×10^4								2.10×10^9
Q: 0-2 Ma	1.09×10^4		8.14×10^3			2.50×10^6		3.30×10^6	
T_2: 2-25 Ma	5.50×10^4		1.21×10^4					1.80×10^8	
T_1: 25-60 Ma	3.40×10^5	1.90×10^6	2.63×10^3					3.82×10^8	
Cr_2: 60-100 Ma	2.03×10^4		6.46×10^2					4.18×10^7	
Cr_1: 100-150 Ma			4.26×10^3					2.76×10^7	1.40×10^{10}
J: 150-210 Ma	2.00×10^4	2.00×10^5	2.59×10^3	2.60×10^5				2.60×10^7	
Tr: 210-245 Ma	1.82×10^5							1.35×10^8	
Pe: 245-290 Ma	7.00×10^3			2.11×10^5					
Cb: 290-354	1.70×10^4	5.50×10^6	5.56×10^3	2.68×10^4				6.19×10^7	
S-D: 354-440 Ma		2.90×10^5	2.34×10^3				3.50×10^7		
Or: 440-500 Ma	2.16×10^4								
Cm: 500-550 Ma	8.13×10^3								
Np: 550-1000 Ma		2.20×10^5	2.30×10^3		1.08×10^4	9.51×10^6		2.28×10^8	3.16×10^{10}
Mp: 1.0-1.6 Ga	3.29×10^4		1.57×10^3					7.61×10^7	
Pp_2: 1.6-2.0 Ga	9.73×10^4	5.44×10^5	2.65×10^3					5.28×10^7	6.20×10^{10}
Pp_1: 2.0-2.45 Ga	1.29×10^4		6.00×10^2	2.22×10^4			4.15×10^9	1.41×10^7	1.42×10^{11}
Ar: 2.45-3.0 Ga	1.46×10^4		5.19×10^4					3.50×10^6	

	Hg	Mn	Mo	Nb	Ni	Pb	PGE	REE	Sb
No date			1.21×10^6						
Q: 0-2 Ma	7.00×10^3				6.33×10^7				
T_2: 2-25 Ma	2.43×10^5		4.07×10^6			1.38×10^7			2.79×10^5
T_1: 25-60 Ma	2.02×10^4	2.21×10^9	1.95×10^9			1.96×10^7			3.98×10^6
Cr_2: 60-100 Ma	3.15×10^4		1.35×10^6						1.58×10^5
Cr_1: 100-150 Ma		4.65×10^8	1.50×10^5	7.87×10^6		1.07×10^7		1.45×10^7	
J: 150-210 Ma			5.31×10^5	3.00×10^7		6.30×10^6		4.00×10^7	4.50×10^6
Tr: 210-245 Ma	5.50×10^5				1.50×10^7	1.26×10^7	6.11×10^3		
Pe: 245-290 Ma	3.37×10^4		1.62×10^5	4.89×10^7		1.70×10^7			5.65×10^5
Cb: 290-354	6.50×10^4					2.46×10^7			2.00×10^5
S-D: 354-440 Ma				6.50×10^6		4.41×10^7		7.50×10^6	2.02×10^5
Or: 440-500 Ma						8.60×10^6		3.60×10^7	2.18×10^5
Cm: 500-550 Ma			3.20×10^5	2.00×10^6		6.49×10^7			
Np: 550-1000 Ma		1.21×10^8				1.44×10^7			
Mp: 1.0-1.6 Ga				8.50×10^6	7.92×10^6	2.10×10^7			
Pp_2: 1.6-2.0 Ga		2.75×10^8			2.56×10^7	5.95×10^7	1.47×10^3		
Pp_1: 2.0-2.45 Ga		4.37×10^9			8.80×10^6		7.67×10^3		
Ar: 2.45-3.0 Ga			1.07×10^5				6.50×10^3		4.46×10^5

	Sn	Th	Ti	U	V	W	Y	Zn	Zr
No date									
Q: 0-2 Ma	1.03×10^7								
T_2: 2-25 Ma	5.00×10^5								
T_1: 25-60 Ma	2.40×10^6							7.00×10^6	
Cr_2: 60-100 Ma						1.10×10^6			
Cr_1: 100-150 Ma		1.16×10^6		2.47×10^5		2.61×10^5			
J: 150-210 Ma	4.82×10^6			6.82×10^5		8.72×10^5	3.00×10^6		2.50×10^7
Tr: 210-245 Ma								4.00×10^7	
Pe: 245-290 Ma	2.50×10^5					1.28×10^6			
Cb: 290-354	2.50×10^6							4.46×10^7	
S-D: 354-440 Ma	4.57×10^5					1.06×10^5		3.37×10^7	2.10×10^8
Or: 440-500 Ma								4.17×10^7	
Cm: 500-550 Ma				3.00×10^5				8.00×10^6	
Np: 550-1000 Ma	2.05×10^6							1.10×10^7	
Mp: 1.0-1.6 Ga	5.00×10^5			1.73×10^6				3.23×10^7	5.00×10^7
Pp_2: 1.6-2.0 Ga								7.67×10^7	
Pp_1: 2.0-2.45 Ga			2.88×10^9	4.84×10^5				8.09×10^6	
Ar: 2.45-3.0 Ga					3.71×10^8			1.18×10^7	

Abbreviations: Ar = Archean; Cb = Carboniferous; Cm = Cambrian; Cr_1 = lower Cretaceous; Cr_2 = upper Cretaceous; J = Jurassic; Mp = Mesoproterozoic; Np = Neoproterozoic; Or = Ordovician; Pe = Permian; PG = PGE; Pp_1 = lower Paleoproterozoic; Pp_2 = upper Paleoproterozoic; Q = Quaternary; RE = REE; S-D = Silurian, Devonian; T_1 = lower Tertiary; T_2 = upper Tertiary; Tr = Triassic

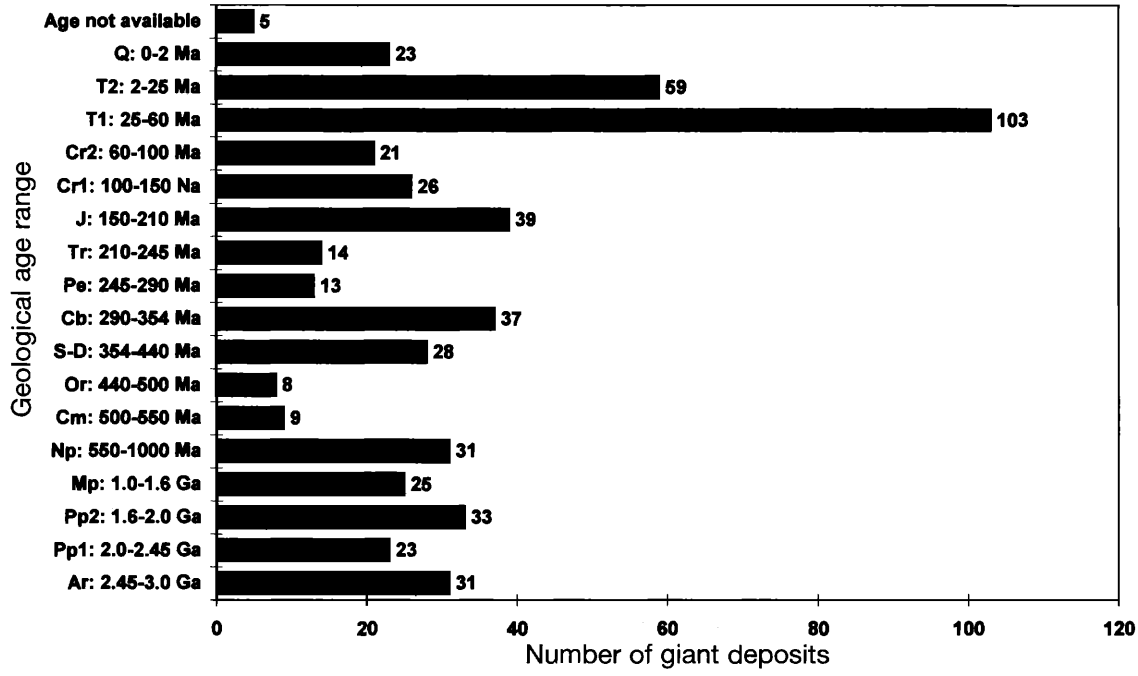

FIG. 6. Giant ore deposits and districts organized by intervals of geologic time during which they formed. Based on data in Tables 9 and 10. Abbreviations: Q = Quaternary; T_1 = lower Tertiary; T_2 = upper Tertiary; Cr_1 = Lower Cretaceous; Cr_2 = Upper Cretaceous; J = Jurassic; Tr = Triassic; Pe = Permian; Cb = Carboniferous; S-D = Silurian, Devonian; Or = Ordovician; Cm = Cambrian; Np = Neoproterozoic; Mp = Mesoproterozoic; Pp_1 = lower Paleoproterozoic; Pp_2 = upper Paleoproterozoic; Ar = Archean.

located at the peak of many of the grade/tonnage graphs that accompany the U.S. Geological Survey mineral deposits models (Cox and Singer, 1986), as well as in graphs for models summarized elsewhere (e.g., Kirkham et al., 1993).

The Witwatersrand basin (Pretorius, 1976) and the Bushveld Complex (von Gruenewaldt et al., 1986) are two outstanding mineralized systems that host a number of giant accumulations, but they are not unique. Lithologic associations similar to the Witwatersrand recognized elsewhere (Armstrong, 1981) host similar types of ore deposits but there is a significant gap between the least endowed major Witwatersrand goldfield (Evander, 1,000 t Au) and the next largest presumed paleoplacer deposit (Tarkwa, Ghana, 530 t Au). M. T. Einaudi (pers. commun., 1998) suggests this gap might indicate a uniqueness of the ore-forming process after all, perhaps an anomalously productive local component of the ore-forming process such as a persistent gold supply from an Au anomalous hinterland (Robb and Meyer, 1990).

An even greater magnitude gap exists between the two large, broadly comparable, magmatic platiniferous horizons: Merensky Reef in the Bushveld Complex (42,000 PGE, calculated geologic tonnage based on 10 ppm PGE/t; Laznicka, 1993, p. 1141) and J-M Reef in the Stillwater Complex (1,159 t PGE reserve, about 6,000 t PGE resource; Todd et al., 1982). Here the extraordinary magnitude of the Bushveld magmatic-stratiform ore accumulations is influenced by the fact that each of the four extensive metalliferous horizons or units have to be treated as a single orebody as there is no geologic justification for subdivision and insufficient data to treat tectonically or erosion-separated segments of the horizons as separate entities. This contrasts with, for example, porphyry copper deposits that enter databases as either single deposits (Bingham Canyon Cu-Mo-Au, Utah) or as geographic clusters or administrative districts (Bingham district). Although database entries in the form of metal accumulating systems would be most desirable, metallogenic system building is in infancy and there is not yet enough data available for a global study.

The strong case for geologic time restriction of certain genetic classes of metallic deposits such as the banded iron-formations (e.g., Cloud, 1973) has been gradually weakened by a growing evidence that cherty banded iron-formations have formed during the Neoproterozoic (the diamictite-associated Rapitan, Jacadigo, Holowilena, and other groups and formations; Laznicka, 1993, p. 903) and the Phanerozoic (the Lahn-Dill Typus of Schneiderhöhn, 1941, 1955), and that small modern analogs of banded iron-formations also exist in the Red Sea (Kimberley, 1989). Similar weakening of a classical interpretation has affected the supposed time-bound character of the pyritic paleoplacers as in the Witwatersrand and in the Quirke syncline, Ontario (Robinson and Spooner, 1984). Force (1991) has identified the great age and its implication for a reducing atmosphere as the only unique factor of the Witwatersrand origin. Great Cainozoic gold placers have formed under oxidizing conditions so it is the pyrite and uraninite only which, if indeed detrital, would be constrained by time. Even if the finding of detrital uraninite in Indus sands (Robinson and Spooner, 1984) and the mineable quantity of detrital pitchblende in till derived from the Key Lake deposits, Saskatchewan (Dahlkamp, 1978), are not considered a strong enough argument against the time-bound origin of Au and U paleoplacers, there is a possibility that the

uranium minerals are postsedimentary, diagenetic or endogenetic, precipitated in depth (e.g., Phillips and Law, 1997).

So what are the remaining candidates of genetic uniqueness among the giant orebodies? Perhaps extraterrestrial materials. Most of the extraterrestrial solids to reach the earth's surface are metalliferous (chondrites have nickel contents of 1.03–1.35% Ni and 3.58 ppm PGE; meteoritic irons are high-grade ores of Fe, Ni, Co, PGE, and Au), but they are received in dispersed form. The largest meteoritic orebody, the Hoba Iron, weighs 60 t and it contains 16.4 percent Ni or nearly 10 t Ni (Mason, 1979). Although several ancient metallic deposits have been, from time to time, interpreted as of meteoritic, impact-assisted, or impact-generated metalizations (Grieve and Masaitis, 1994), only in Sudbury, Ontario, the debate for (e.g., Stöffler et al., 1994) and against (e.g., Card et al., 1984) continues, although the prevalent opinion favors impact-related structural preparation followed by magma ascent and magmatogene Ni-Cu ore separation (Eckstrand, 1996). Lightfoot et al. (1997) have demonstrated that >80 percent of the 1.85 Ga Sudbury magma types is of crustal derivation with the rest probably derived from the mantle, but this does not provide sufficient evidence for meteoric origin of the Sudbury Ni-Cu-PGE ore (estimated at 1.55 bt grading 1.2 Ni, 1.09% Cu, 0.4 g/t Pt, and 0.4 g/t Pd).

Are the local superaccumulations of metals controlled more by the site of present occurrence, or by a process that could proceed almost anywhere? Both alternatives exist as end members, but in most cases the truth is in between. Modern research on ore deposits indicates almost without exception that ore formation is the end result of a multistage, prolonged formational sequence moving in the right direction. Although some hydrothermal ore types such as porphyry Cu-Mo deposits show statistically significant association with certain broad geotectonic settings (e.g., subductive continental margins; Sawkins, 1990), the actual ore sites occupy a fraction of the eligible area, are controlled by magma derivation and by fractionation in magma chambers, and are emplaced without regard to the wall and roof rocks of the mineralized intrusion (Titley, 1993; Keith and Swan, 1996). Clark (1993) found no specific attributes at Chuquicamata and El Teniente that might aid in the identification of other outsize deposits and tentatively suggested the protracted magmatic history with limited arc migration as the main factors that enhance (but do not determine) the formation of giant metal accumulations. On the opposite side of the genetic spectrum are metalized provinces that are highly enriched, at the present level of exposure and probably also in depth, in certain metals, as in W and Sb in east-central China (Jiangxi, Guizhou, and Hunan; Li Yidou, 1993). There, a variety of ore types and many generations of the same metal has resulted, although the strongest mineralization that includes giant deposits is associated with a particular magmatic series, in the Jiangxi tungsten province with peraluminous biotite granite and leucogranite.

Can the location of future giant deposits be scientifically predicted and exploration programs directed exclusively toward finding a giant, bypassing the smaller deposits ? The answer is no. If most giant deposits are magnitude peaks of ore types that consist of mixed-size populations, the chance of finding giants is statistical and it increases as more smaller deposits are found. However, exploration preference should be directed to areas that permit its occurrence. There are, however, numerous case histories of the discovery of giant deposits that do not support the above philosophy (Laznicka, 1997), as the discovery of the Carajas Fe province (Machamer et al., 1991), Muruntau Au deposit (Kudrat Sabirov, oral commun., 1993), Olympic Dam Cu-U-Au deposit (Reeve et al., 1990), and Voisey's Bay Ni-Cu deposit (Ramshaw, 1995). None of these finds was a succesful outcome of a project designed, from the onset, to find a giant deposit of the type that was actually discovered, although some projects came close. Exploration for the ore giants is really like a fishing expedition (Laznicka, 1996b); you fish where the right fish is expected to be, and one of them might be big!

Acknowledgments

This paper is an outcome of the author's involvement with the International Geological Correlation Project 354, and the support received is gratefully acknowledged. Also acknowledged is the 1997 Gledden Travel Fellowship from the University of Western Australia supported by David Groves that funded my stay in the Centre for Teaching and Research in Strategic Minerals in Nedlands. This contribution has been substantially improved by suggestions from M.T. Einaudi and two anonymous *Economic Geology* referees.

April 6, 1998; February 4, 1999

REFERENCES

Abdullayev, K.M., 1964, Ore petrographic provinces: Moscow, Nedra, 135 p. (in Russian).

Armstrong, F.C., ed., 1981, Genesis of uranium and gold-bearing Precambrian quartz-pebble conglomerates: U.S. Geological Survey Professional Paper 1161-A, 28 sections.

Bailey, E.H., and Everhart, D.L., 1964, Geology and quicksilver deposits of the New Almaden district, Santa Clara County, California: U.S. Geological Survey Professional Paper 360, 270 p.

Barton, M.D., 1996, Granitic magmatism and metallogeny of southwestern North America: Royal Society of Edinburgh Transactions, Earth Sciences, v. 87, p. 261–280.

Barton, P.B., Jr., 1983, Unconventional mineral deposits: A challenge to geochemistry, *in* Shanks, W.C., III, ed., Cameron volume on unconventional mineral deposits: New York, American Institute of Mining Engineers, p. 1–14.

Bercé, B., 1958, Geology of the mercury deposit Idrija: Geologija, Ljubljana, v. 4, p. 5–62 (in Serbo-Croatian).

Bilibin, Y.A., 1955, Basics of placer geology: Akademiia Nauk SSSR Doklady, 471 p. (in Russian).

Blevin, P.L., and Chappell, B.V., 1992, The role of magma series, oxidation states and fractionation in determining the granite metallogeny of eastern Australia: Royal Society of Edinburgh Transactions, Earth Sciences, v. 83, p. 305–317.

Bornhorst, T.J., Paces, J.B., Grant, N.K., Obradovich, J.D., and Huber, N.K., 1988, Age of native copper mineralization, Keweenaw peninsula, Michigan: Economic Geology, v. 83, p. 619–625.

Brimhall, G.H., and Crerar, D.A., 1989, Ore fluids, magmatic to supergene: Reviews in Mineralogy, v. 17, p. 235–282.

Burnham, C.W., 1979, Magmas and hydrothermal fluids, *in* Barnes, H.L., ed., Geochemistry of hydrothermal ore deposits: New York, Wiley Interscience, p. 71–136.

Candela, P.A., 1989, Magmatic ore-forming fluids: Thermodynamics and mass transfer calculations of metal concentrations: Reviews in Economic Geology, v. 4, p. 203–221.

Card, K.D., Gupta, V.K., McGrath, P.H., and Grant, F.S., 1984, The Sudbury structure: Its regional geological and geophysical setting: Ontario Geological Survey Special Volume 1, p. 25–43.

Carlin, W.D., Jr., 1985, Indium: Mineral facts and problems, 1985 edition: U.S. Bureau of Mines Bulletin 675, p. 369–376.

Clark, A.H., 1993, Are outsize porphyry copper deposits either anatomically or environmentally distinctive? Society of Economic Geologists Special Publication 2, p. 213–283.

——ed., 1995, Giant ore deposits II: Kingston, Ontario, Queens University, 540 p.

Cloud, P.E., 1973, Paleoecological significance of the banded iron-formation: ECONOMIC GEOLOGY, v. 68, p. 1135–1143.

Colvine, A.C., 1989, An empirical model for the formation of Archean gold deposits: Products of final cratonization of the Superior province, Canada: ECONOMIC GEOLOGY MONOGRAPH 6, p. 37–53.

Cox, D.P., and Singer, D.A., eds., 1986, Mineral deposit models: U.S. Geological Survey Bulletin 1693, 379 p.

Dahlkamp, F.J., 1978, Geological appraisal of the Key Lake U-Ni deposits, northern Saskatchewan: ECONOMIC GEOLOGY, v. 73, p. 1430–1449.

Dessau, G., 1977, Die Quecksilber- und Antimonlagerstätten den Toskana: Freiberger Forschungshefte, Reihe C, no. 328, p. 47–71 (in German).

Duckworth, R.C., Shanks, W.C., III., Teagle, D.A.H., and Zierenberg, R.A., 1998, High grade sediment-hosted sulfide deposits on the seafloor: Society of Economic Geologists Newsletter 32, p. 20–21.

Eckstrand, O.R., 1996, Nickel-copper sulphide: Geological Society of America, Geology of North America, v. P-1, p. 584–606.

Erickson, R.L., 1973, Crustal abundance of elements and mineral reserves and resources: U.S. Geological Survey Professional Paper 820, p. 21–25.

Ferrell, J.E., 1985, Lithium: Mineral facts and problems: U.S. Bureau of Mines Bulletin 675, p. 461–470.

Fersman, A.E., 1933, Geochemistry: Collected works of the Academician A.Ye. Fersman: Moscow, U.S.S.R., Academy of Sciences, 1960, v. 1 and 2, 913 p. (in Russian).

Force, E.R., 1991, Placer deposits: Reviews in Economic Geology, v. 5, p. 131–140.

Fountain, R.C., and Hayes, A.W., 1979, Uraniferous phosphate resources of the southeastern United States: U.S. Department of Energy Publication GJBX-110 (79), p. 65–122.

Fyfe, W.S., Price, N.J., and Thompson, A.B., 1978, Fluids in the crust: Amsterdam, Elsevier, 383 p.

Goldfarb, R.J., Snee, L.W., and Pickthorn, W.J., 1993, Orogenesis, high-T thermal events, and gold vein formation within metamorphic rocks of the Alaskan Cordillera: Mineralogical Magazine, v. 57, p. 375–394.

Grieve, R.A.F., and Masaitis, V.L., 1994, The economic potential of terrestrial impact craters: International Geology Review, v. 36, p. 105–151.

Groves, D.I., Goldfarb, R.J., Gebre-Mariam, M., Hagemann, S.G., and Robert, F., 1997, Orogenic gold deposits: A proposed classification in the context of their crustal distribution and relationship to other gold deposit types: Ore Geology Reviews, v. 134, p. 7–28.

Guilbert, J.M., and Park, C.F., Jr., 1986, The geology of ore deposits: New York, Freeman, 985 p.

Henley, R.W., and Adams, J., 1979, On the evolution of giant gold placers: Institute of Mining and Metallurgy Transactions, v. 89, p. B41–B49.

Herzig, P.M., and Hannington, M.D., 1995, Polymetallic massive sulfides at the modern seafloor. A review: Ore Geology Reviews, v. 10, p. 95–115.

Jébrak, M., and Hernandez, A., 1995, Tectonic deposition of mercury in the Almaden district, Las Cuevas deposit, Spain: Mineralium Deposita, v. 30, p. 413–423.

Keith, S.B., 1986, Petrochemical variations in Laramide magmatism and their relationships to Laramide tectonic and metallogenic evolution in Arizona and adjacent regions: Arizona Geological Society Digest, v. 16, p. 89–101.

Keith, S.B., and Swan, M.M., 1996, The great Laramide porphyry cluster of Arizona, Sonora and New Mexico: The tectonic setting, petrology and genesis of a world-class porphyry metal cluster: Geology and Ore Deposits of the American Cordillera Symposium, Geological Society of Nevada, Reno, Proceedings, v. 3, p. 1667–1747.

Keith, S.B., Laux, D.P., Maughan, G., Schwab, K., Ruff, S., Swan, M.M., Abbott, E.W., and Friberg, S., 1991, Magma series and metallogeny, a case study from Nevada and environs: Nevada Geological Society Field Trips Guidebook, v. 1, p. 404–493.

Kimberley, M.M., 1989, Exhalative origins of iron formations: Ore Geology Reviews, v. 5, p. 13–145.

Kirkham, R.V., Sinclair, W.D., Thorpe, R.I., and Duke, J.M., eds., 1993, Mineral deposit modelling: Geological Association of Canada Special Paper 40, 770 p.

Kramer, D.A., 1985, Magnesium: Mineral facts and problems: U.S. Bureau of Mines Bulletin 675, p. 471–482.

Krupp, R.E., and Seward, T.M., 1987, The Rotokawa geothermal system, New Zealand: An active epithermal gold-depositing environment: ECONOMIC GEOLOGY, v. 82, p. 1109–1129.

Kuck, P.H., 1985, Vanadium: Mineral facts and problems, 1985 edition: U.S. Bureau of Mines Bulletin 675, p. 895–915.

Laznicka, P., 1973, Development of non-ferrous metal deposits in geologic time: Canadian Journal of Earth Sciences, v. 19, p. 18–25.

——1983, Giant ore deposits: A quantitative approach: Global Tectonics and Metallogeny, v. 2, no. 1-2, p. 41–63.

——1985a, Empirical metallogeny: Amsterdam, Elsevier, 1794 p.

——1985b, Data on ore deposits: A critical review of their sources, acquisition, organization and presentation, *in* Wolf, K.H., ed., Handbook of stratabound and stratiform ore deposits: Amsterdam, Elsevier, v. 11, p. 1–118.

——1989, Derivation of giant ore deposits [abs.]: International Geological Congress, 28th, Washington, D.C., Abstracts Volume 2, p. 2–268.

——1993, Precambrian empirical metallogeny: Amsterdam, Elsevier, 1622 p.

——1997, Discovery of giant metal deposits and districts: International Geological Congress, 30th, Beijing, Proceedings, p. 355–366.

——1998a, The setting and affiliation of giant ore deposits: Quadrennial International Association on the Genesis of Ore Deposits Symposium, 9th, Proceedings, p. 1–14.

——1998b, Design of an international data base of giant metal accumulations: Global Tectonics and Metallogeny, v. 6, no. 3, p. 1–10.

Le Bas, M.J., 1987, Nephelinites and carbonatites: Geological Society of London Special Publication 30, p. 53–83.

Lightfoot, P.C., Keays, R.R., Morrison, G.G., Bite, A., and Farrell, K.P, 1997, Geochemical relationships in the Sudbury Igneous Complex: Origin of the Main Mass and offset dikes: ECONOMIC GEOLOGY, v. 92, p. 289–307.

Lindgren, W., 1933, Mineral deposits, 4th ed.: New York, McGraw-Hill, 930 p.

Livingston, D.L., Mauger, R.L., and Damon, P.E., 1968, Geochronology of the emplacement, enrichment, and preservation of Arizona porphyry copper deposits: ECONOMIC GEOLOGY, v. 63, p. 30–36.

Li Yidou, 1993, Poly-type model for tungsten deposits and vertical structural zoning model for vein-type tungsten deposits in South China: Geological Association of Canada Special Paper 40, p. 555–568.

Machamer, J.F., Tolbert, G.E., and L'Esperánce, R. L., 1991, The discovery of Serra dos Carajas: ECONOMIC GEOLOGY MONOGRAPH 8, p. 275–285.

Mason, B., 1979, Data on geochemistry, 6th ed.: U.S. Geological Survey Professional Paper 440-B-1, 132 p.

McCarthy, T.S., 1994, A review of the regional structural controls on the occurrence and character of the Ventersdorp contact reef: Economic Geology Research Unit Witwatersrand University Information Circular 276, 21 p.

McKelvey, V.E., 1960, Relation of reserves of the elements to their crustal abundances: American Journal of Science, v. 258-A, p. 234–241.

Meyer, C., 1981, Ore-forming processes in geologic history: ECONOMIC GEOLOGY 75TH ANNIVERSARY VOLUME, p. 6–41.

Myers, R.E., McCarthy, T.S., and Stanistreet, I.G., 1990, A tectono-sedimentary reconstruction of the development and evolution of the Witwatersrand basin, with particular emphasis on the Central Rand Group: South African Journal of Geology, v. 93, p. 180–201.

Naldrett, A.J., 1989, Magmatic sulfide deposits: New York-Oxford, Clarendon Press, 186 p.

Nelson, C.H., and Hopkins, D.H., 1972, Sedimentary processes and distribution of particulate gold in the northern Bering Sea: U.S. Geological Survey Professional Paper 689, 27 p.

Nikiforov, N.A., 1976, Central Asia mercury province and mercury-bearing zones of Kazakhstan, *in* Smirnov, V.I., Kuznetsov, V.A., and Fedorchuk, V.P., eds., Metallogeny of mercury: Moscow, Nedra, p. 155–165 (in Russian).

Oreskes, N., and Einaudi, M.T., 1990, Origin of rare earth element-enriched hematite breccias at the Olympic Dam Cu-U-Au-Ag deposit, Roxby Downs, South Australia: ECONOMIC GEOLOGY, v. 85, p. 1–28.

Ozerova, N.A., 1981, New mercury ore belt in western Europe: Geologiya Rudnykh Mestorozhdenii, no. 6, p. 49–56 (in Russian).

Paone, J., 1970, Germanium: Mineral facts and problems: U.S. Bureau of Mines Bulletin 650, p. 563–571.

Peabody, C.E., and Einaudi, M.T., 1992, Origin of petroleum and mercury in the Culver-Baer cinnabar deposit, Mayacmas district, California: ECONOMIC GEOLOGY, v. 87, p. 1078–1103.

Pesonen, P.E., Tuillis, E.L., and Zinner, P., 1949, Missouri Valley manganese deposits, South Dakota: U.S. Bureau of Mines Report of Investigations 4375, 90 p.

Petkof, B., 1985, Gallium, in Mineral Facts and Problems: U.S. Bureau of Mines Bulletin 675, p. 291–296.
Phillips, G.N., and Hughes, M.J., 1996, The geology and gold deposits of the Victorian gold province: Ore Geology Reviews, v. 11, p. 255–302.
Phillips, G.N., and Law, D.M., 1997, Hydrothermal origin for Witwatersrand gold: Society of Economic Geologists Newsletter 31, p. 26–33.
Phillips, G.N., Groves, D.I., and Kerrich, R., 1996, Factors in the formation of the giant Kalgoorlie gold deposit: Ore Geology Reviews, v. 10, p. 295–317.
Plunkert, P.A., 1985, Thallium: Mineral facts and problems, 1985 ed.: U.S. Bureau of Mines Bulletin 675, p. 829–834.
Pohl, W., 1992, W. and W.E. Petrascheck's Lagerstättenlehre, 4. Auflage: Stuttgart, Schweizerbart'sche Verlagsbuchhandlung, 504. p. (in German).
Pretorius, D.A., 1976, The nature of the Witwatersrand gold-uranium deposits, *in* Wolf, K.H., ed., Handbook of strata-bound and stratiform ore deposits: Amsterdam, Elsevier, v. 7, p. 29–62.
Ramshaw, D., 1995, Voisey Bay: Mining Magazine, November 1995, p. 276–279.
Reeve, J.S., Cross, K.C., Smith, R.N., and Oreskes, N., 1990, Olympic Dam copper-uranium-gold-silver deposit, *in* Hughes, F.E., ed., Mineral deposits of Australia and Papua New Guinea: Melbourne, Australasian Institute of Mining and Metallurgy, p. 1009–1035.
Robb, L.J., and Meyer, F.M., 1990, The nature of the Witwatersrand hinterland: Conjectures on the source area problem: ECONOMIC GEOLOGY, v. 85, p. 511–536.
Robinson, A., and Spooner, E.T.C., 1984, Can the Elliot Lake uraninite-bearing quartz-pebble conglomerates be used to place limits on the oxygen content of the Early Proterozoic atmosphere?: Geological Society of London Journal, v. 141, p. 221–228.
Rona, P.A., and Scott, S.D., 1993, A special issue on sea-floor hydrothermal mineralization: New perspectives: Preface: ECONOMIC GEOLOGY, v. 88, p. 1933–1974.
Routhier, P., 1963, Les Gisements Metalifères: Géologie et Principes de Recherche: Paris, Mason, 1,283 p. (in French).
——1980, Où Sont les Métaux pour L'avenir?: Bureau de Recherches Géologiques et Minière Mémoires 105, 410 p. (in French).
Rudnick, R.L., and Fountain, D.M., 1995, Nature and composition of the continental crust: A lower crustal perspective: Reviews of Geophysics, v. 33, p. 267–309.
Rytuba, J.J., ed., 1993, Active geothermal systems and gold-mercury deposits in the Sonoma-Clear Lake volcanic fields: Society of Economic Geologists Guidebook Series, v. 16, 361 p.
——1996, Cenozoic metallogeny of California: Geology and Ore Deposits of the American Cordillera Symposium, Geological Society of Nevada, Reno, Proceedings, p. 803–822.
Rytuba, J.J., and Glanzman, R.K., 1979, Relation of mercury, uranium and lithium deposits to the McDermitt caldera complex, Nevada-Oregon: International Association on the Genesis of Ore Deposits Symposium, 5th, Proceedings, v. 2, p. 109–117.
Samoilov, V.S., 1984, Geochemistry of carbonatites: Moscow, Nauka, 190 p. (in Russian).
Saupe, F., 1990, Geology of the Almadén mercury deposit, Province of Ciudad Real, Spain: ECONOMIC GEOLOGY, v. 85, p. 482–510.
Sawkins, F.J., 1990, Metal deposits in relation to plate tectonics, 2nd ed.: New York, Springer Verlag, 461 p.
Schneiderhöhn, H., 1941, Lehrbuch der Erzlagerstättenkunde: Stuttgart, Enke Verlag, v. 1, 858 p. (in German).
——1955, Erzlagerstätten: Jena, Fischer Verlag, 375 p. (in German).
Scott, J., Collins, G.A., and Hodgson, G.W., 1954, Trace metals in the McMurray oil sands and other Cretaceous reservoirs of Alberta: Canadian Mining and Metallurgy Bulletin for January 1954, p. 34–42.
Shaw, A.L., and Guilbert, J.M., 1990, Geochemistry and metallogeny of Arizona peraluminous granitoids with reference to Appalachian and European occurrences: Geological Society of America Special Paper 246, p. 317–356.
Sillitoe, R.H., 1993, Giant and bonanza gold deposits in the epithermal environment: Assessment of potential genetic factors: Society of Economic Geologists Special Publication 2, p.125–156.
Sinclair, B., 1989, Lake Rotokaua sulphur deposit: Australasian Institute of Mining and Metallurgy Monograph 13, p. 89–91.
Singer, D.A., 1995, World-class base and precious metal deposits: A quantitative analysis: ECONOMIC GEOLOGY, v. 90, p. 88–104.
Smirnov, V.I., 1976, Geology of mineral deposits: Moscow, Mir, 520 p.
Smith, G.I., 1979, Subsurface stratigraphy and geochemistry of late Quaternary evaporites, Searles Lake, California: U.S. Geological Survey Professional Paper 1043, 130 p.
Smith, J.W., and Milton, C., 1966, Dawsonite in the Green River Formation of Colorado: ECONOMIC GEOLOGY, v. 61, p. 1029–1042.
Sorensen, H., ed., 1974, The alkaline rocks: New York, Wiley, 622 p.
Stöffler, D., Deutsch, A., Avermann, M., Bischoff, L., Brockmeyer, P., Bühl, P., Lakomy, R., and Müller-Mohr, V., 1994, The formation of the Sudbury structure, Canada: Toward a unified impact model: Geological Society of America Special Paper 293, p. 303–318.
Taylor, S.R., 1964, Abundance of chemical elements in the continental crust: Geochimica et Cosmochimica Acta, v. 28, p. 1280–1281.
Taylor, S.R., and McLennan, S.M., 1995, The geological evolution of the continental crust: Reviews of Geophysics, v. 33, p. 241–265.
Titley, S.R., 1993, Characteristics of porphyry copper occurrence in the American Southwest: Geological Association of Canada Special Paper 40, p. 433–464.
Todd, S.G., Keith, D.W., LeRoy, L.W., Schissel, D.J., Mann, E.L., and Irvine, T.N., 1982, The J-M platinum-palladium reef of the Stillwater Complex, Montana: I. Stratigraphy and petrology: ECONOMIC GEOLOGY, v. 77, p. 1454–1480.
Urabe, T., 1985, Aluminous granite as a source of hydrothermal ore deposits: An experimental study: ECONOMIC GEOLOGY, v. 80, p. 148–157.
Von Gruenewaldt, G., Hatton, C.J., and Merkle, R.K.W., 1986, Platinum-group element-chromitite associations in the Bushveld Complex: ECONOMIC GEOLOGY, v. 82, p. 1067–1079.
Wallis, D.S., and Oakes, G.M., 1990, Heavy mineral sands in eastern Australia, *in* Hughes, F.E., ed., Mineral deposit of Australia and Papua New Guinea: Melbourne, Australasian Institute of Mining and Metallurgy, p. 1599–1608.
Wedepohl, K.H., 1995, The composition of the continental crust: Geochimica et Cosmochimica Acta, v. 59, p. 1217–1232.
Whiting, B.H., Hodgson, C.J., and Mason, R., eds., 1993, Giant ore deposits: Society of Economic Geologists Special Publication 2, 404 p.
Wilson, M., 1989, Igneous petrogenesis: A global tectonic approach: London, Unwin Hyman, 466 p.
Wooley, A.R., 1989, The spatial and temporal distribution of carbonatites, *in* Bell, K., ed., Carbonatites, genesis and evolution: London, Unwin Hyman, p. 15–37.
Xie Xuejing, 1995, The surficial geochemical expression of giant ore deposits, *in* Clark, A.H., ed., Giant ore deposits II: Kingston, Queen's University, p. 476–485.
Youngson, J.H., and Craw, D., 1995, Evolution of placer gold deposits during regional uplift, central Otago, New Zealand: ECONOMIC GEOLOGY, v. 90, p. 731–745.